# HARPI - A new weather radar display

by Isztar I. Zawadzki

A thesis submitted to the Faculty of Graduate Studies and Research in partial fulfilment of the requirements for the degree of Master of Science.

Department of Meteorology - McGill University.

## ABSTRACT

For HARPI, a weather radar antenna scans routinely in azimuth and (slowly) in elevation, as for CAPPI. The range is divided into uniform intervals of a few miles. For each interval, the maximum signal in the few-mile range interval is displayed against vertical and horizontal coordinates of elevation and azimuth, and so of height and circumferential distance. This gives, for one interval, a horizontal strip, of small extent in the vertical. Many such strips are displayed one above the other, for progressively increasing range, in a Height-Azimuth-Range Position Indicator.

Display equipment using a cathode-ray tube and Polaroid camera proved successful through half a hail season at Penhold, Alberta. In this thesis, sample pictures are scrutinized, and circuits are shown and described, with detailed treatment in appendices. The three-dimensional pattern of a hailstorm is recreated from HARPI sections, and it is concluded that HARPI plus one CAPPI or other map make an excellent combination.

HARPI - A new weather radar display. by I.I. Zawadzki

# HARPI - A new weather radar display

by

Isztar I. Zawadzki

A thesis submitted to the Faculty of Graduate Studies and Research in partial fulfilment of the requirements for the degree of Master of Science.

Department of Meteorology
McGill University
Montreal

April 1968

© Isztar I. Zawadzki 1969

## Acknowledgments

The writer is greatly indebted to Professor J. S. Marshall for his helpful guidance and advice during every stage of the present work. Professor K.L.S. Gunn's continuous encouragement is particularly appreciated. Mr. Ernest Ballantyne's assistance in the design and testing of the electronics described here was of utmost importance. Without his collaboration this work would not have been possible.

The fruitful discussions with members of the Stormy Weather Group are acknowledged as well as their help during the preparation of this thesis.

The writer appreciates the assistance from Miss Ursula Seidenfuss who drafted most of the diagrams, and from Miss Arlene Milburn and Miss Suzette Milburn who typed the draft copies and the final manuscript.

HARPI - A new weather radar display


## ABSTRACT

For HARPI, a weather radar antenna scans routinely in azimuth and (slowly) in elevation, as for CAPPI. The range is divided into uniform intervals of a few miles. For each interval, the maximum signal in the few-mile range interval is displayed against vertical and horizontal coordinates of elevation and azimuth, and so of height and circumferential distance. This gives, for one interval, a strip of much less extent in the vertical. Many such strips are displayed one above the other, for progressively increasing range, in a Height-Azimuth-Range Position Indicator. Display equipment using a cathode-ray tube and Polaroid camera has been built and used through half a hail season at Penhold, Alberta. Sample pictures are scrutinized in this work, and circuits are shown and described, with detailed treatment in appendices. From one set of HARPI sections, other sections are obtained for a hailstorm, which is described in detail.

Table of contents


| | | |
|---|---|---|
| | ABSTRACT | |
| | ACKNOWLEDGMENTS | |
| 1. | INTRODUCTION | 1 |
| 2. | PROGRAMME FOR ROUTINE SCANNING BY THE ANTENNA OF A WEATHER RADAR | 5 |
| 3. | HEIGHT AZIMUTH RANGE POSITION INDICATOR | 8 |
| 4. | HARPI IN ALBERTA, SUMMER 1967 | 13 |
| 5. | RESULTING PICTURES | 17 |
| 6. | THE INTEGRATOR | 23 |
| 7. | HARPI CIRCUITRY | 31 |
| 8. | RANGE RESOLUTION OF THE DISPLAY | 33 |
| 9. | DESCRIPTION OF THE STORM OF 28 JULY 67 AT 1706-1709 | 40 |
| 10. | EVALUATION OF PRESENTATIONS OF RADAR DATA | 46 |
| 11. | CONCLUSIONS | 54 |
| | REFERENCES | 58 |
| | APPENDICES | 60 |

## 1. Introduction

Weather radar as a detector of precipitation can (and should) be used for many purposes: operationally for short term forecasts for the general public, for aviation, hydrology and other things, and also as a research tool for better understanding of the processes involved in the evolution of storms. Operational needs determine to a certain extent the direction of research, and as research progresses the operations can be expanded and improved.

Because radar is an expensive instrument a single unit often has to serve both purposes. Therefore the form in which the information is obtained and (later) presented must be designed for both the above requirements. The antenna program which determines the way in which the radar beam scans the space, and the final display of the data obtained have to be considered.

For a long time, information about the vertical structure of the storm has been obtained either by vertical scanning at a fixed bearing displaying the information in height-range coordinates (the RHI* presentation); or by pointing the antenna vertically with the information appearing in height-time coordinates. Under a steady state assumption (a good approximation in winter situations) the time coordinate can be converted into a range coordinate, knowing the velocity with which the storm moves. With a horizontal structure of primary interest, radar antennae have been programmed to rotate horizontally at some fixed elevation, usually close to zero degrees, to yield the well-known Plan Position Indicator (PPI) presentation. The information generally has been displayed on a CRT scope and photographed. Intensity measurements

*RHI: Range-Height-Indicator

have been obtained by stepping up or down the radar gain or by using the A scope. With no integration of the signal performed prior to feed to the CRT, a grainy texture on the pictures has resulted, due to the fluctuating nature of meteorological echoes.

From this early stage substantial progress has been made. The technique of iso-echo contours was developed by Atlas (1947, 1953). Kodaira (1959) built an electronic integrator of the radar signal and its output was used by Niessen and Geotis (1963) to produce a five-level iso-echo contour on a PPI* display.

The concept of a 5-dimensional presentation was developed at McGill University as a means of satisfying both the operational and the research requirements. An antenna program consisting of rapid horizontal rotation and slow elevation was devised to scan 3-dimensional space. The information obtained first was processed optically to produce constant altitude PPI's (Marshall, 1957). Later an electronic system to produce these CAPPI* maps was developed (East and Dore, 1957). The information was stored on film with the density of the film proportional to the intensity level of the target. Wein (1964) went further than this and by a scanning process produced what is presently the output of the McGill radar: six CAPPI layers produced by a facsimile machine (local or remote) with the intensity level quantized in steps of 10 db and represented by shades of gray on the facsimile paper. The 3-dimensions of space, the intensity of the targets and time are the five dimensions of the radar information.

*PPI: Plan-Position-Indicator
CAPPI: Constant Altitude PPI

Other similar displays have been built. A system with digital output, called STRADAP*, is described by Sweeney (1961). It presents intensities in 6 db steps on a CAPPI map in addition to a similar map containing maximum heights in 10 kft intervals.

The CAPPI concept is to be regarded as an extension of the zero-degree PPI to many levels; the horizontal dimension is emphasized by the display while the recognition of the vertical structure requires extra effort.

The present work describes a new type of display in which the presentation emphasizes the vertical dimension in such a manner as to retain the advantages of RHI or vertically pointed antenna without losing the five-dimensional characteristic.

*STRADAP: STorm RAdar DAta Processor

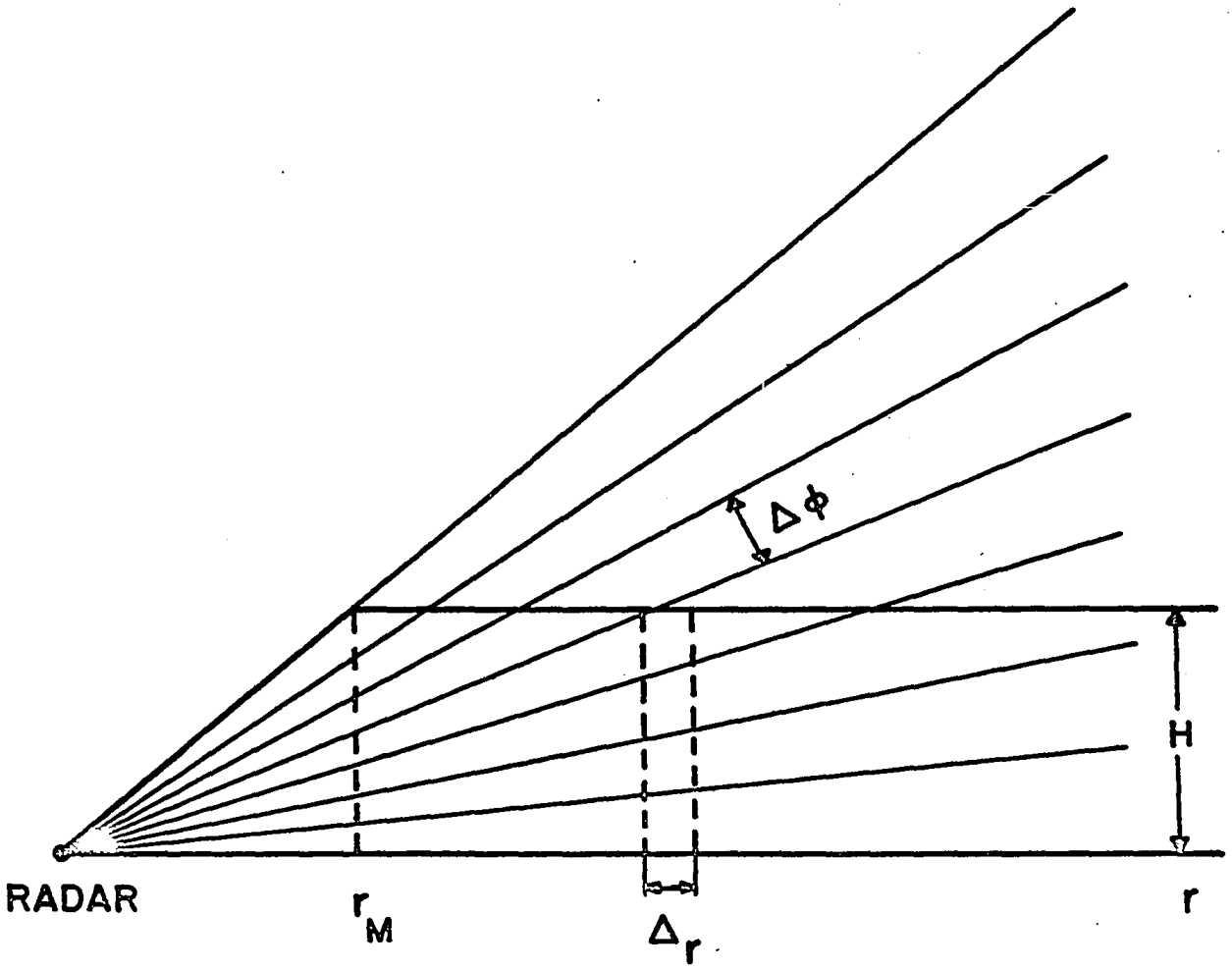


Figure 1 – Vertical section of an antenna program. The radial lines are the axes of successive radar beams; $r_M$ is the minimum range at which the height H is covered by such program.

## 2. Programme for Routine Scanning by the Antenna of a Weather Radar

Precipitation, which is the principal target of weather radars, decreases with height, above 20 kft, in frequency and intensity. For any given climate, a layer of atmosphere can be chosen extending a few tens of thousands of feet upward from the surface, such that the precipitation pattern almost never extends beyond the top surface of the layer. For H, the layer-thickness, 40 kft seems to be adequate in Alberta, 50 kft is almost enough in Montreal, and for parts of the United States a value of 70 kft might be required (Henry, 1964; Jordan, 1961).

This layer in which precipitation occurs can be covered by a routine cyclical scanning programme of the radar antenna. There is practical advantage in a programme such as that illustrated in Figure 1, in which the azimuth angle $\theta$ increases at a constant rate through some 20 revolutions, while the angle of elevation $\phi$ increases slowly from zero or a small positive angle to a maximum elevation $\phi_M$ of $20^\circ$ or more. (With $\phi_M < \pi/2$, a "cone of silence" is left above the radar; for $\phi_M$ between $20^\circ$ and $30^\circ$ the cone of silence is acceptably small and the period of the scanning cycle is made shorter by a factor of 3 or more than the time needed to scan all heights at all ranges.) From $\phi_M$ the elevation $\phi$ can return to $\phi = 0$ during one further revolution in azimuth and become ready for the start of a new cycle. Letting $\Delta\phi$ be the change in $\phi$ during one revolution in azimuth, it is simple and useful to keep $\Delta\phi$ constant (apart from the rapid return) and approximately equal to the beamwidth.*

---

*While there is in fact a continuous variation in sensitivity with off-axis angle, it is convenient in the present context to work in terms of a beam with an abrupt drop in sensitivity and intensity at some angle (about $\frac{1}{2}^\circ$) off the axis of the beam.

Letting $\phi_H$ denote the angle subtended at the radar by the layer-thickness H, then at range r we have

$$\phi_H \approx H/r \qquad (1)$$

If the elevation changes by some small amount $\Delta\phi$ with each rotation in azimuth, then

$$n = \phi_H/\Delta\phi \approx H/r\ \Delta\phi \qquad (2)$$

where n is the number of rotations in azimuth required to irradiate the layer from the horizontal up to height H above the horizon, at range r.

We have taken $\phi_M$ as a maximum angle of elevation. We can take a related maximum value for n, and denote it by $n_M$. The total number of revolutions will be $n_M + 1$, allowing one revolution for the elevation to return to zero, and

$$n_M = \phi_M/\Delta\phi \qquad (3)$$

Substituting $n_M$ into (2), we obtain a value for r which we shall denote by $r_M$:

$$n_M \approx H/r_M\ \Delta\phi$$

$$r_M \approx H/n_M\ \Delta\phi \qquad (4)$$

In a way, $r_M$ is a minimum value of r; specifically, $r_M$ is the smallest value of r at which the scanning programme reaches to height H. At range $r_M$ the scanning programme just reaches to height H, and at smaller angles the height of coverage is proportional to the range.

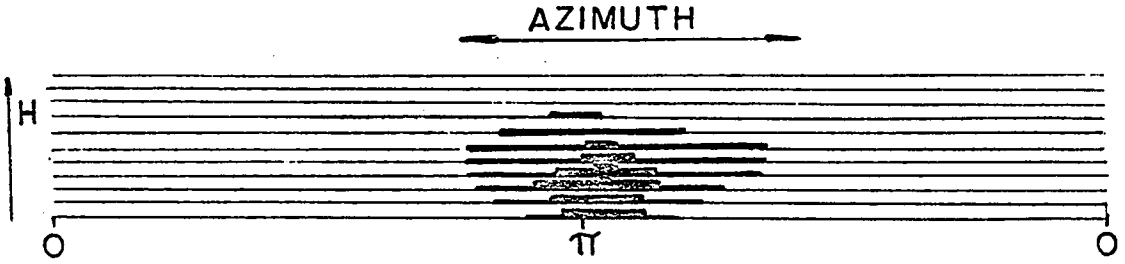


Figure 2 - HARPI section. Here the thickness of the line instead of its brightness indicates the intensity of the echo.

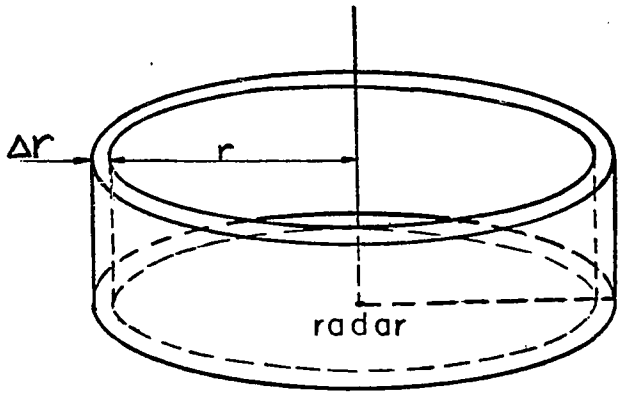


Figure 3

3. Height Azimuth Range Position Indicator

HARPI stands for Height-Azimuth-Range-Position-Indicator. This weather-radar display is made up of between 10 and 100 sections such as that shown in Figure 2. Each section describes the precipitation at all azimuths in a short range interval $\Delta r$. Each rotation of the antenna is accompanied by the writing of one almost horizontal line, along which the shade of grey indicates the maximum target intensity in the short range interval from r to $r + \Delta r$.

The space reported upon in a single HARPI section is of course a cylindrical annulus as shown in Figure 3. The abscissae are either azimuth or distance along the circumference of a circle of radius r. On the latter basis, both ordinate (height) and azimuth represent distances. If the reproductions are both to the same scale, there is no distortion in the representation of the cylindrical slice through the storm, except for the opening-up of the cylinder. Experience indicates an advantage, however, in stretching the height of the storm by a factor 2 relative to the scale of horizontal distance.

The number of near-horizontal lines in the HARPI section is the number n already discussed, and varies inversely with r:

$$n \approx H/r\ \Delta\emptyset \qquad (2)$$

In going from one HARPI section to many, covering many successive range intervals, we have kept constant the spacing of the lines, so that the height of the picture section varies inversely as the range, whereas the height H that is depicted is invariant with range (Figure 4a). We

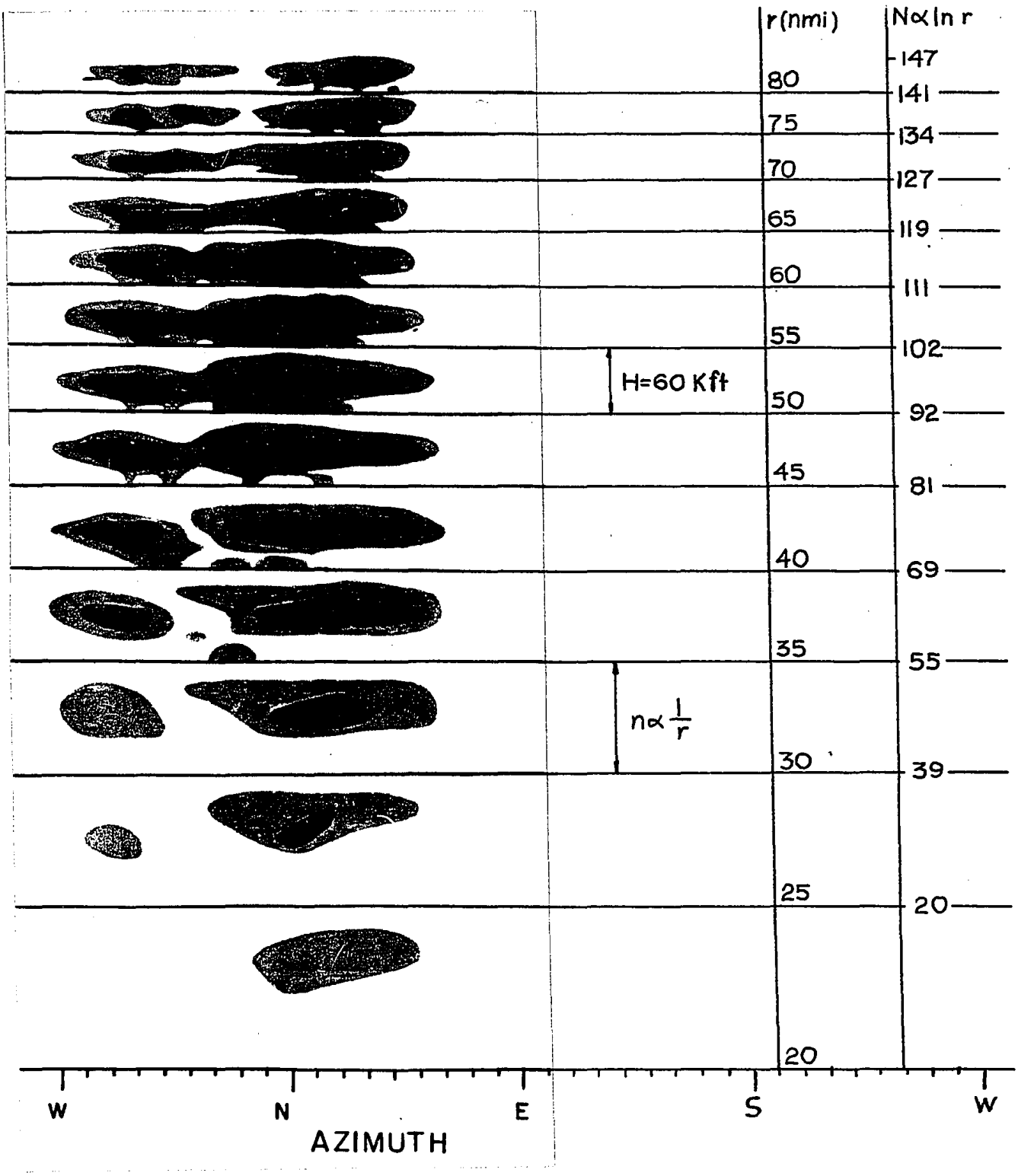


Fig. 4a - Handmade HARPI of 2057 EST, 18 July 1964

have kept constant the width of the picture-section, representing azimuth $\theta$ or circumferential distance $2\pi r\theta$. Thus the scales of reproduction of height and circumferential distance both vary in the same way with range. As a result, the same shape factor between horizontal and vertical scales, be it 1:1 or 2:1 or anything else, is maintained at all ranges.

Successive range intervals are taken all the same size. It is intended that successive sections shall appear one above the other on an axis of N (number of lines, Figure 4a), although we have not yet had success with the circuitry for this.

$$\Delta N = n \approx H/r \quad \Delta\phi \tag{5}$$

If we take a succession of equal increments $\Delta r$, the proportionality between $\Delta N$ and $r^{-1}$ becomes

$$\Delta N \propto \frac{\Delta r}{r} = \Delta \log r \tag{6}$$

therefore

$$N \propto \log r \tag{7}$$

and so the scale of N that is linear in N (number of lines) is at the same time a logarithmic scale of range.

In displaying the radar information in discrete increments of range, the question arises as to what intensity parameter should represent each range interval. The average of the echoes in a range interval is convenient in some cases (like water budget studies), while the maximum of them is more significant from the point of view of storm physics. Moreover, taking into account that the maxima are not recoverable from the average, but that inversely, the average can be estimated from a display where the maxima are presented, we have chosen this last possibility.

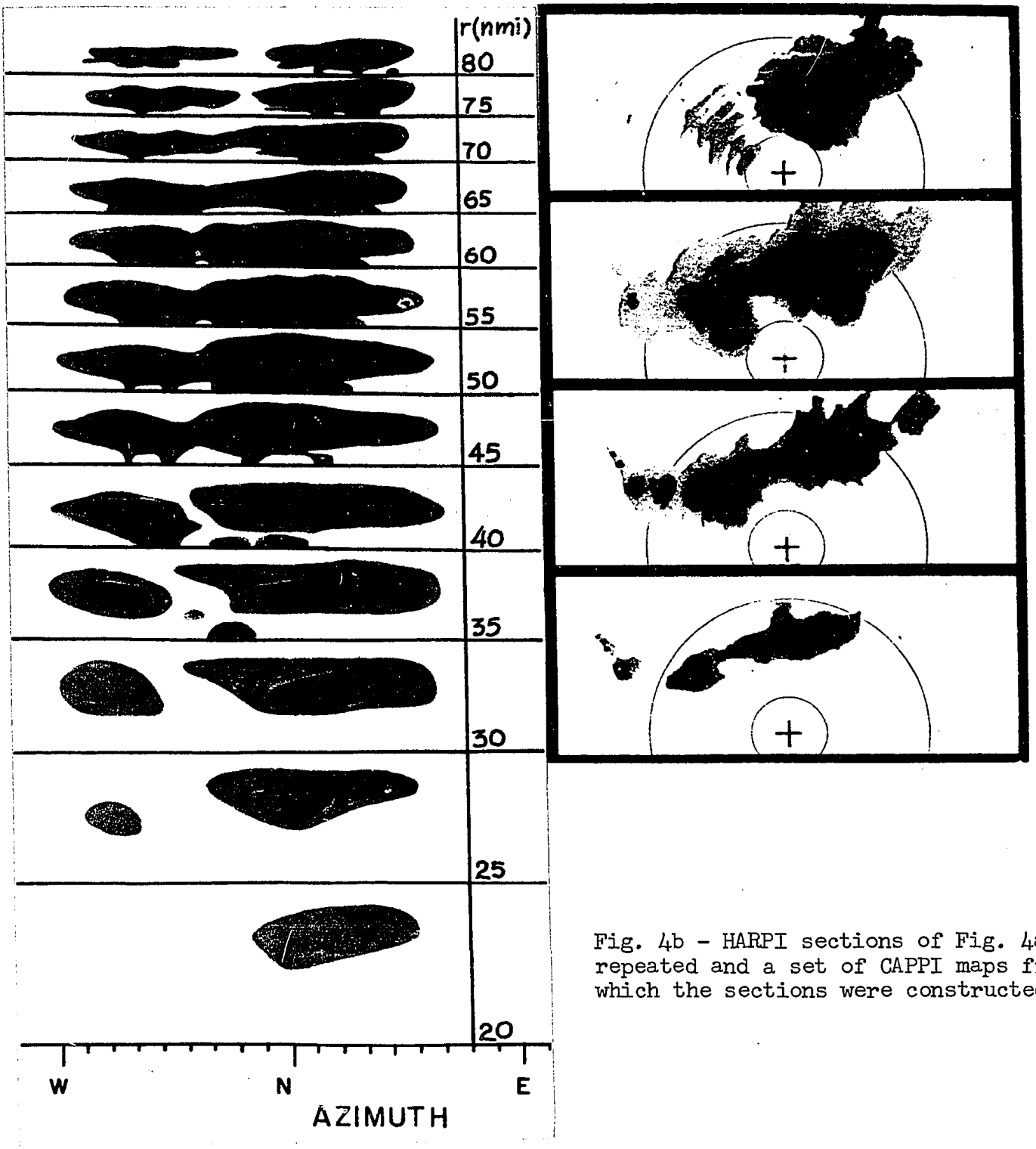


Fig. 4b - HARPI sections of Fig. 4a repeated and a set of CAPPI maps from which the sections were constructed.

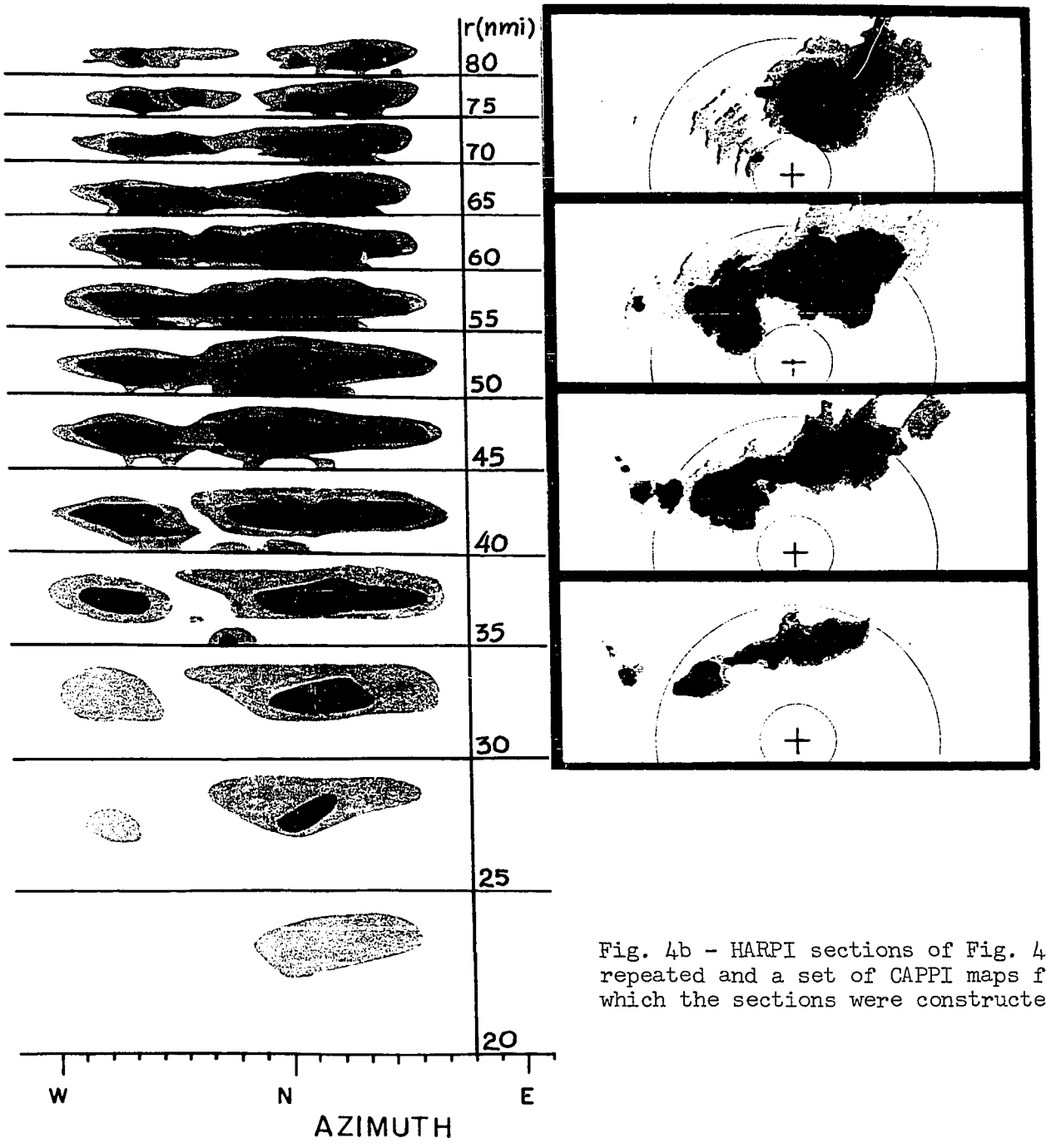


Fig. 4b - HARPI sections of Fig. 4a repeated and a set of CAPPI maps from which the sections were constructed.

In Fig. 4b, the right-hand portion is the set of CAPPI maps corresponding to 5, 15, 30, 40 kft which were used to obtain the HARPI sections. These CAPPI maps were selected from the routine output of the CPS-9 radar which operates at Montreal Airport, although the situation displayed here has been studied intensively by Holtz (1968).

Briefly, the CPS-9 radar is used to generate 6 pairs of CAPPI maps every $22\frac{1}{2}$ minutes. A 60 db range of target intensity is displayed on each map of a pair in quantized grey shades, each representing a step of 20 db in received power. One member of each pair (shown in Fig. 4b) contains shades 1, 3 and 5 and the other map shades 2, 4 and 6 so that intensity steps of 10 db can be read from a pair of maps. The six CAPPI heights are 5, 10, 15, 20, 30, 40 kft during the summer season. The shades used to construct the HARPI sections were 1, 2, 5, 6.

To obtain these pictures from the set of CAPPI's, circles with radius increasing by steps of 5 nmi were drawn; then the maximum width of each shade in the 5-nmi interval was determined and the angle subtended by it was plotted in rectangular height-azimuth coordinates with each annulus of the CAPPI contributing to a different HARPI section; a smooth line was traced to join the plotted values, extrapolating where necessary. The circles on the CAPPI's indicate the extreme ranges shown on the HARPI display.

Although the HARPI sections were drawn by hand from data contained only in four pairs of CAPPI maps (and therefore not taking full advantage of the capabilities of the HARPI display), many features become more apparent by examining the HARPI sections. The storm is divided in two distinct bodies; the increase in area with height results in an overhang extending in all directions; the rate of change of area with height appears clearly in the HARPI's. In general the vertical structure of the storm is the dominating feature of the new display.

## 4. HARPI in Alberta, Summer 1967

The FPS-502 radar at Penhold is provided and maintained by NRC for use in the Alberta Hail Studies and has the following characteristics:

| | | | |
|---|---|---|---|
| Wavelength | 10.4 cm | Pulse length | 1.75μsec |
| Peak Power | 250 kW | PRF | 480 Hz |

This radar is used with a custom-built antenna (beam-width $1.15^{\circ}$) and pedestal. The antenna rotates in azimuth ($\theta$) at a rate of 8 rev $min^{-1}$, while its programme in elevation ($\phi$) has the following 3-minute cycle:

From $\theta = 90^{\circ}$ (points east), $\phi = 0^{\circ}$,

$\phi$ increasing $1^{\circ}$ per revolution in $\theta$, for 20 revs, then

$\phi$ constant at $20^{\circ}$ for 1 revolution (from $\theta = 90^{\circ}$)

$\phi$ dropping from $20^{\circ}$ to $0.5^{\circ}$ in 1 revolution

$\phi$ recovering from $-0.5^{\circ}$ to $0.0^{\circ}$ in 1 revolution

$\phi$ constant at $0^{\circ}$ for 1 revolution.

One PPI photograph is taken on 35 mm film for each revolution in azimuth; these photographs have been the permanent record for many years and will probably continue to be so. Other PPI photographs are taken less frequently with a Polaroid camera for operational use.

During the period July 24 to Aug 25 1967, Polaroid HARPI's were taken on an experimental basis. Fourteen sections were presented on every picture, each corresponding to a range interval $\Delta r = 2$ nmi. The

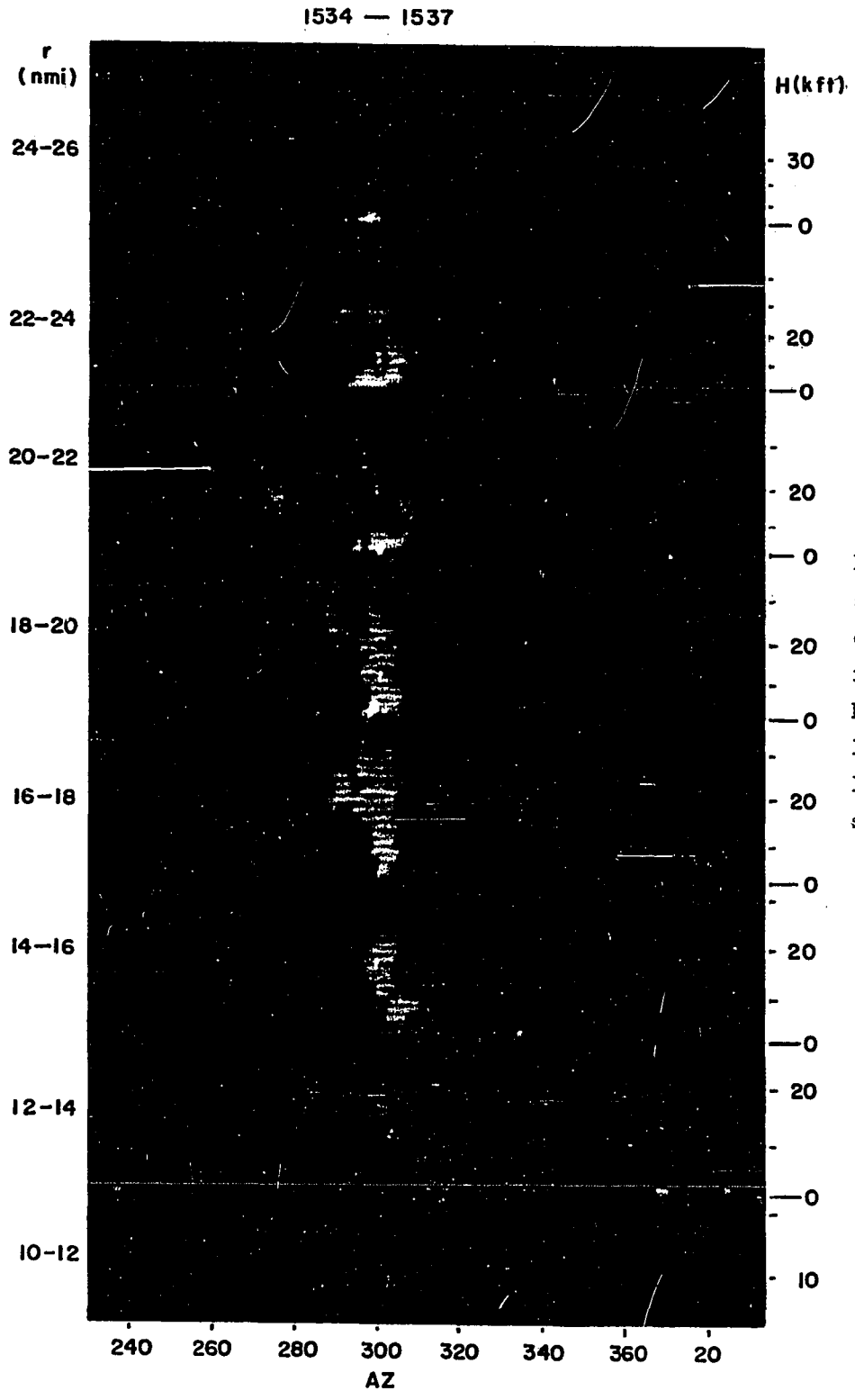


Fig. 5 - Eight HARPI sections of the storm of 28 July 1967 at its early stage. Note the overhang at 18-20 nmi at the left-hand side of the storm.

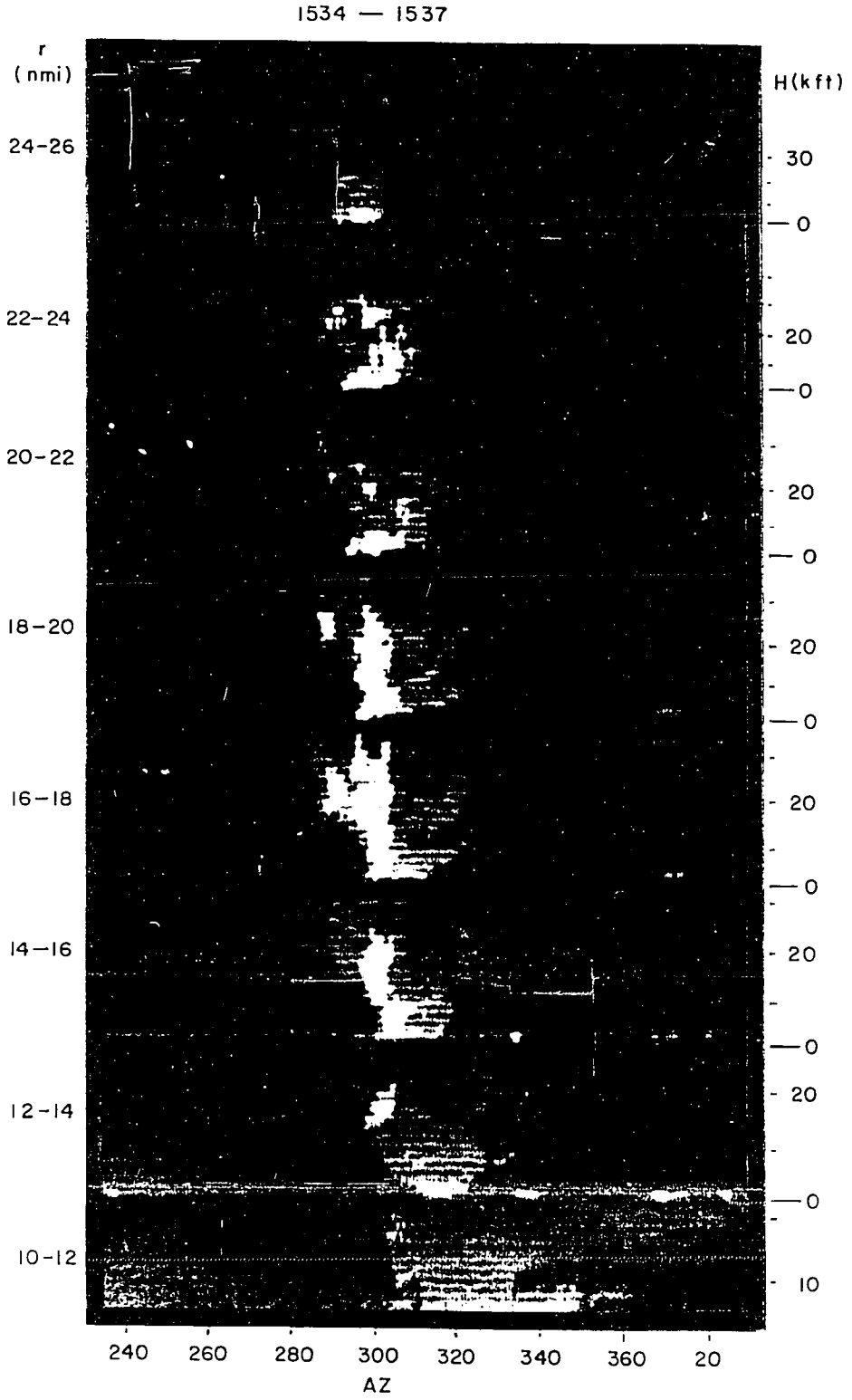


Fig. 1 - Radar RHI sections of the storm of 28 July 1967 at its early stage. Note the overhang at 14-16 and at the left-hand side of the storm.

minimum range was adjustable in steps of 5 nmi from 10 nmi to 35 nmi. Therefore intervals of 28 nmi in the range 10-63 nmi could be covered. Fig. 5 is one such HARPI picture.

In the radar-covered region the storms normally begin their life cycle in the NW-SW quadrant and travel toward the eastern side of the area, passing close to Penhold. Accordingly the range setting was changed several times during each storm. The pictures were taken every 3 minutes when the storms were very active, and at longer time intervals during the less active initial and final stages. A total of 53 hours of record (about 800 pictures) and 12 storm-occasions resulted from the operation. The shortest record covered 30 minutes and the longest 9 hours.

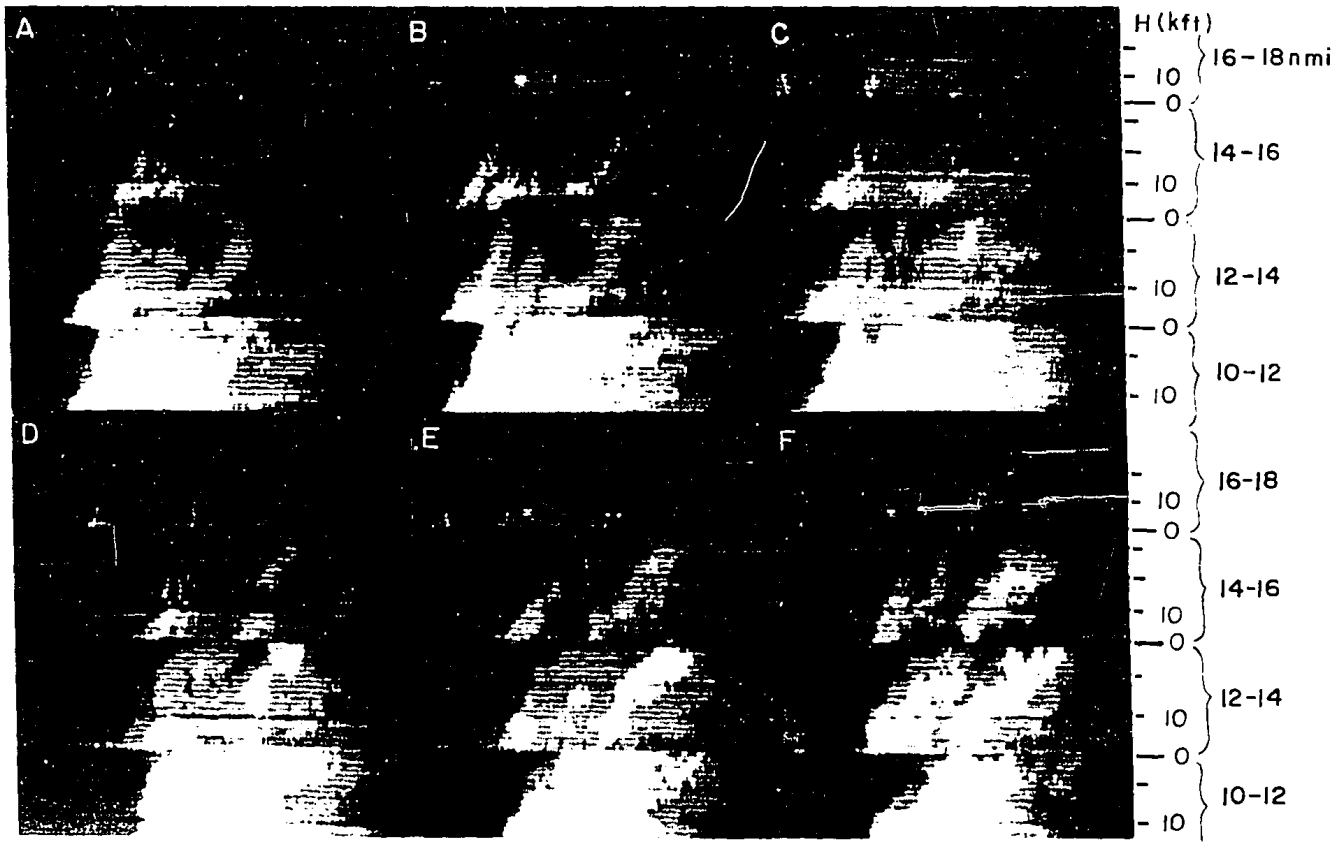


Fig. 6a (top)

Sequence of 6 HARPI sections taken every 3 min, in the time interval 1633-1651 during the storm on 28 July '67. It shows a mature stage of the storm, with the main body being inside the 10 nmi radius, and therefore not present in the HARPI sections.
Note the sloping cell at 12-14 nmi at the right-hand side of the storm. The sequence shows its development in intensity: in B, a small region of shade 3 appears aloft and in subsequent pictures it spreads and joins the low level precipitation of the same intensity.

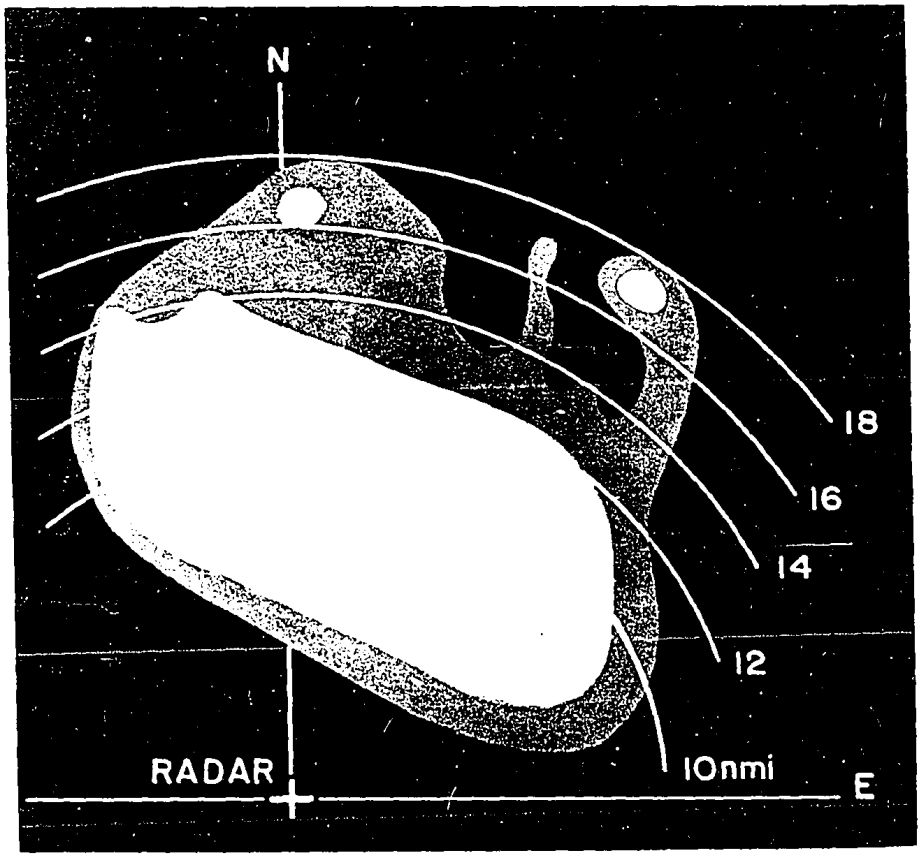


Fig. 6b (left)

Hand-made zero-degree PPI constructed from the picture labelled C in Fig. 6a.

5. Resulting Pictures

The best example of the use of the new display was on 28 July 67 even though the range was uncomfortably short. The storm that day produced the first echo at 43 nmi and NW from the radar. It passed just to the north during its most active stage.

In Fig. 6a portions of 6 polaroid pictures, taken at 3-minute intervals, have been assembled. Each one of the pictures labelled A, B, C, D, E, F extends in azimuth from bearing 320° to bearing 90° and has 4 range intervals (10-12, 12-14, 14-16, 16-18 nmi). A possible plan geometry at 0° elevation is shown in Fig. 6b, constructed from the bottom lines of the HARPI sections in the picture labelled C of Fig. 6a. Limits of HARPI range intervals are indicated by circles every two miles.

An example of the integration employed may be seen where 2 small portions of shade 2 just cross into the 14 to 16 mile range interval. These appear clearly in the HARPI photograph owing to the retention by the Integrator of the peak signal to represent the entire range interval.

HARPI pictures portray angles linearly, which is to say that the same height interval represents one degree of elevation at all ranges, and the same interval of width represents one degree of azimuth at all ranges. (The height interval is twice the width interval, for a shape factor 2:1.) The height scales shown in Fig. 6a are calculated from $H = r \tan \phi$ and so they are different for each range interval. However, circumferential distance is also proportional to range so that the 2:1 factor is maintained in linear dimensions as well.

Because the antenna elevation angle increases smoothly with time the azimuth, lines on the HARPI pictures should actually be inclined to the horizontal by one degree for each 360° of azimuth. In Fig. 6a the difference in elevation angle is 0.36° from one side to the other. The height scale drawn opposite the horizontal lines on Fig. 6a is therefore correct only at the centre of each picture.

Reverting to the discussion favouring presentation of the maximum signal, the need of choice between maximum and average appears again when we consider the problem of integration of meteorological echoes in order to reduce its characteristic fluctuations. It has been shown by Smith (1966) that taking the maxima out of many independent values of intensity levels (logarithm of intensity) reduces the fluctuations by approximately the same amount as averaging them*. Therefore the selection of the maxima has two effects: reveals the intense regions of the storm and reduces the fluctuations of the signal. The data used for this integration come from different half-pulse lengths (integration in range) and different pulses (with the antenna continuously rotating this represents integration in time and azimuth). With a pulse length of 1.75 μsec there are 15 independent samples in $\Delta r$ = 2 nmi. According to Smith's calculations, this integration alone would reduce the fluctuations to a standard deviation $\sigma$ = 1.6 db. On the other hand, the integration in time-azimuth was performed over 8 pulses which with the PRF of 480 Hz results in a time lapse of 1/60 sec = 16.5 msec between the first and last pulse. This is less than the usually accepted time for independence (the order of 50 msec for

*Actually taking maxima is better than averaging intensity levels for a number of data less than ten and worse for a larger number, although the differences are only of the order of 0.2 db. Neither of them is as good as averaging intensities, but the limited dynamic range of our integrator restricts us from using this possibility.

$\lambda$ = 10 cm (Bartnoff, Paulsen and Atlas, 1952; Hitschfeld and Dennis, 1956)). On the other hand, in our case, the independence is also achieved through change in azimuth, which with the antenna rotation rate of 8 rpm is 0.8 degrees in 1/60 sec, a value smaller than but comparable to the beam-width. Assuming that in this condition the two extreme pulses give independent returns while the 6 others are partially dependent, the overall integration would reduce the fluctuations to a value of $\sigma$ = 1.3 db. Due to the fact that $\sigma$ decreases slowly if the number of independent samples is greater than $\sim$ 10, further integration is not justifiable because the reduction in $\sigma$ is made at the cost of space resolution. The intensity level values are quantized in steps of 10 db after integration; thus the standard deviation of each threshold is 1.3 db.

It can be observed on the HARPI pictures that the boundaries between shades are not smooth and, furthermore, isolated units of a given shade appear surrounded by the immediate lower shade. This "noisiness" of the pictures could be due to the remaining fluctuations. A region in which the intensity level is close enough to a threshold could produce a noisy picture even if the intensity level is completely uniform throughout this region.

The other possible explanation is that the storm is actually noisy in the sense that at a given instant the distribution in space of the intensity level has small scale components with an amplitude of a few db superimposed on a more gradual variation. By taking the maxima out of many samples these components were made visible, while the average would smooth them out. Of course, both effects (incomplete integration and noisiness of nature) could contribute to the noisiness of the pictures.

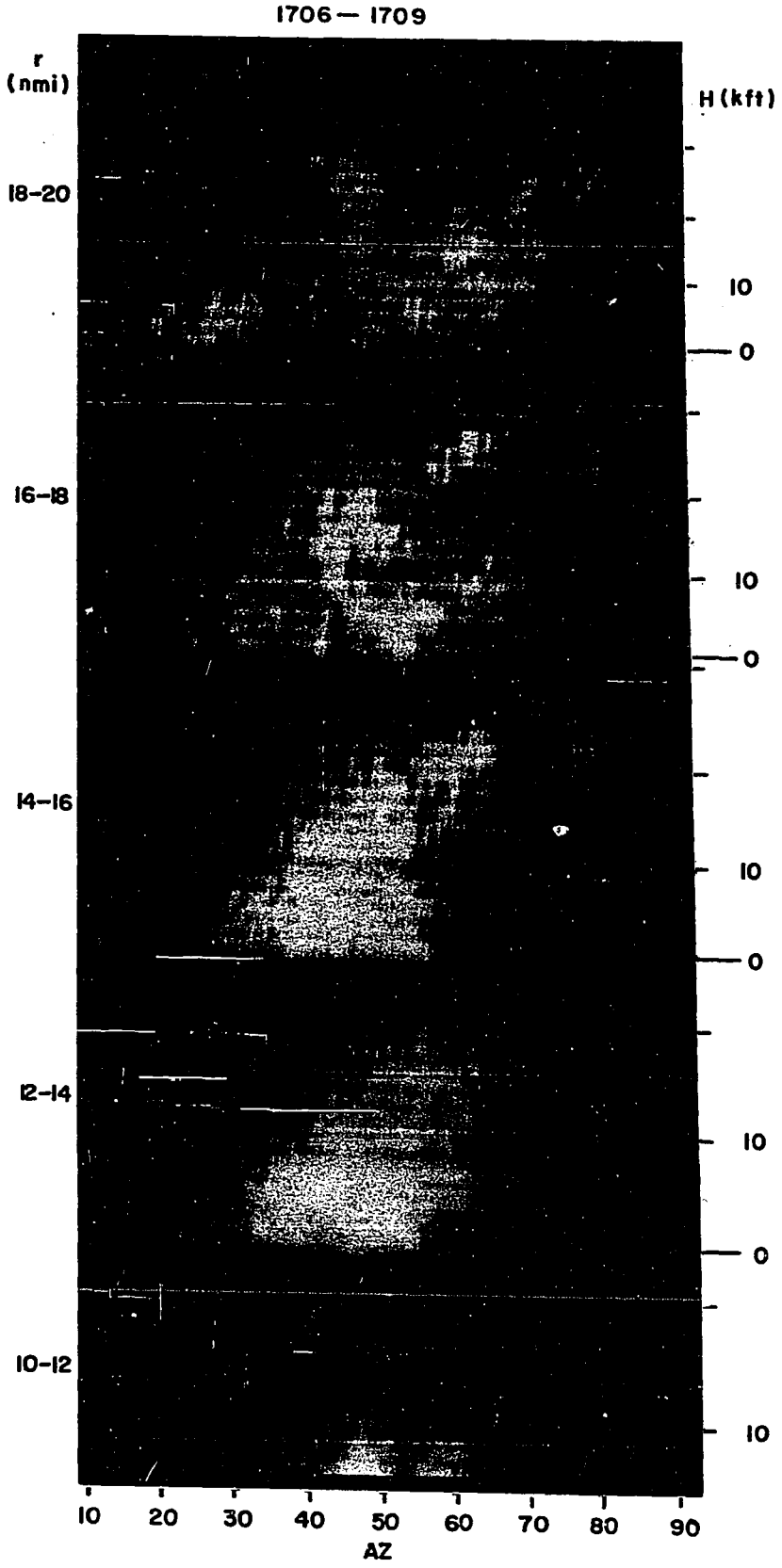


Fig. 7 - Five HARPI sections of the same storm at a late stage. Note that the overhang (now at 16-18 nmi) is at the right-hand side of the storm. This is due to the geometry of the HARPI: a feature which is located in the SW side of a storm will appear at the left-hand side of the picture when the storm is in the NW quadrant, and will be at its right-hand side after the storm moves to the NE quadrant.

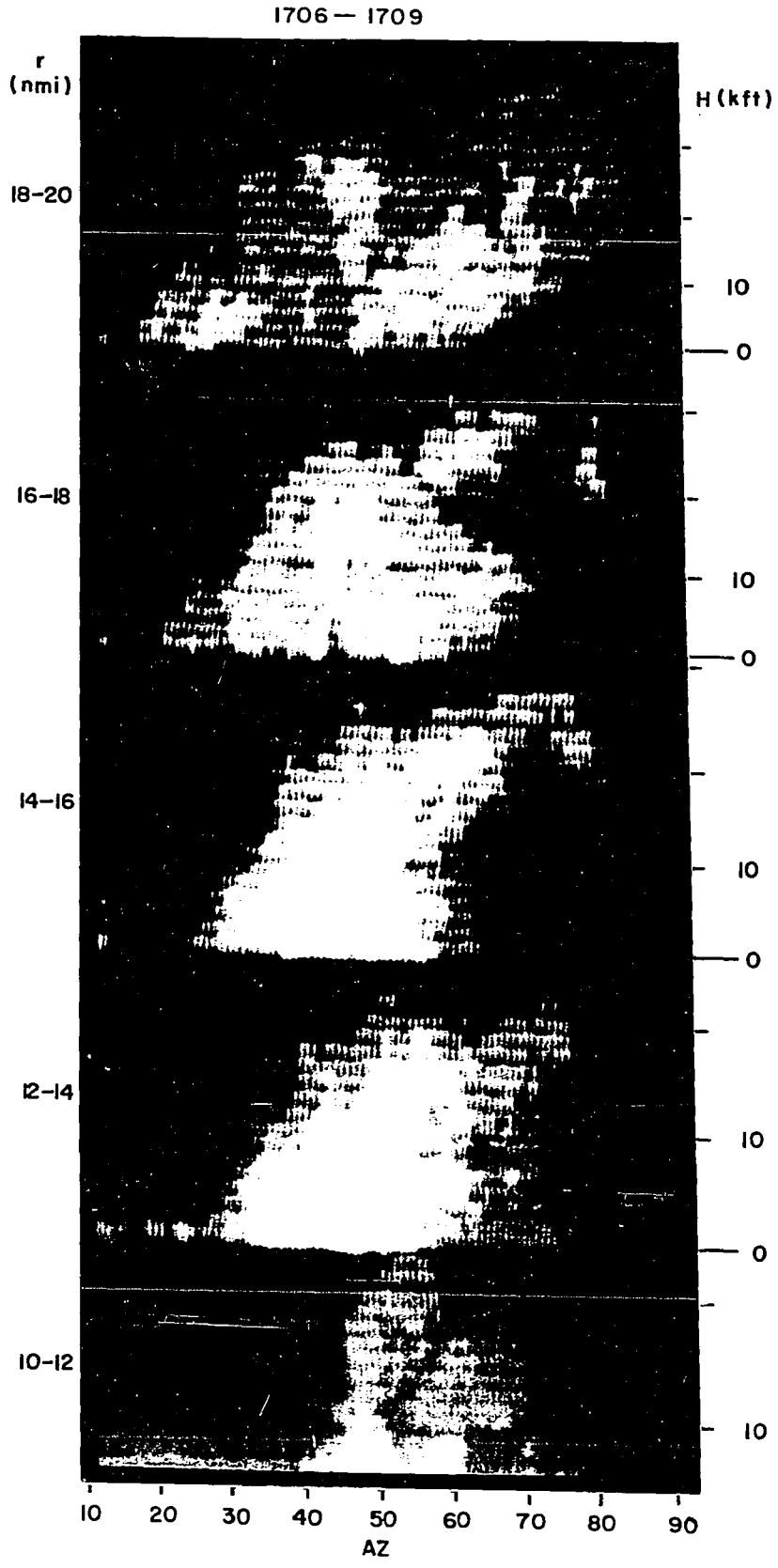


Fig. 7 -- Five HARPI sections of the same storm at a late stage. Note that the overhang (now at 16-18 nmi) is at the right-hand side of the storm. This is due to the geometry of the HARPI: a feature which is located in the SW side of a storm will appear at the left-hand side of the picture when the storm is in the NW quadrant, and will be at its right-hand side after the storm moves to the NE quadrant.

A close inspection of the pictures (see Figure 7) reveals that they are composed of horizontal rows of little vertical lines which are the elementary units of the pictures. Each unit represents 1 degree in vertical elevation and 0.8 degrees in azimuth at every range. This is therefore the resolution of the presentation.

Some limitations of the pictures (mentioned again later in the descriptions of the circuits) are as follows:

a) There are fluctuations along the height axis in the position of the elementary units. Although their amplitude is only a fraction of the vertical dimension of the units, the fluctuations degrade the quality of the picture. They should not be confused with variation in the elevation angle of the antenna.

b) The brightness is not constant along the vertical extent of the elementary units. Related to that, the shape of the units is not rectangular but shows a "tear-drop" form. For the darker shades this results in a separation between the horizontal lines.

c) The vertical spacing of the horizontal lines is not uniform and so a partial overlapping between two of them may occur while a wider gap is left below. Although there is no loss of information, the quality of the picture is again affected.

d) The length of the azimuth axis was not always constant during a single antenna cycle, resulting (for about one-third of the pictures) in curved edges at the right-hand side of the pictures. The variation could reach, in some cases, a length equivalent to 5 degrees in azimuth. This irregularity was embarrassing because it produced artificial sloping of the storms when it appeared.

The halation produced by the writing spot on the CRT, so troublesome in quantitative radar displays, was not apparent on the pictures because of the prior integration and a good separation between the grey scale thresholds.

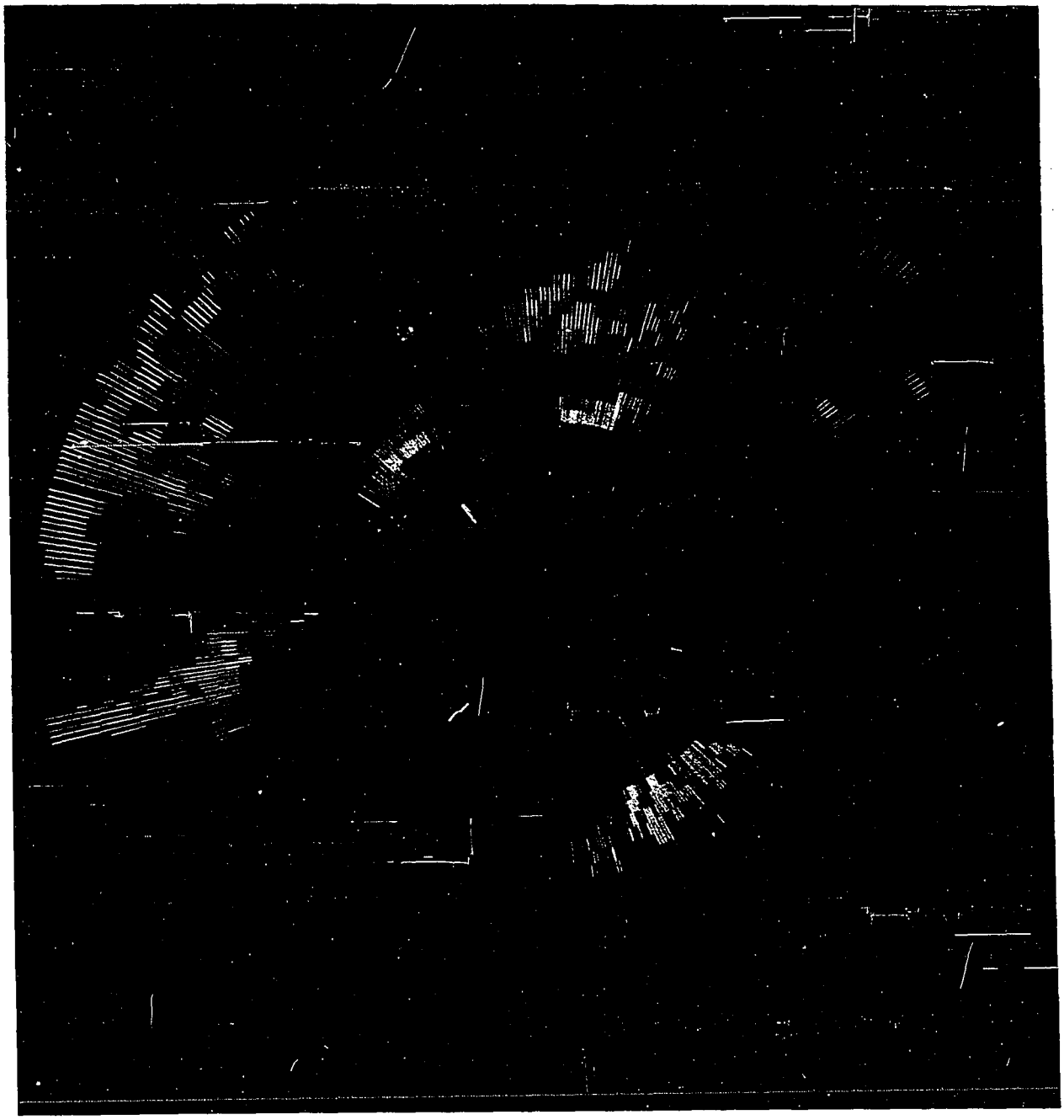

Fig. 8 - PPI picture using video integrated over 2 nmi in range and over ~1 degree in azimuth.

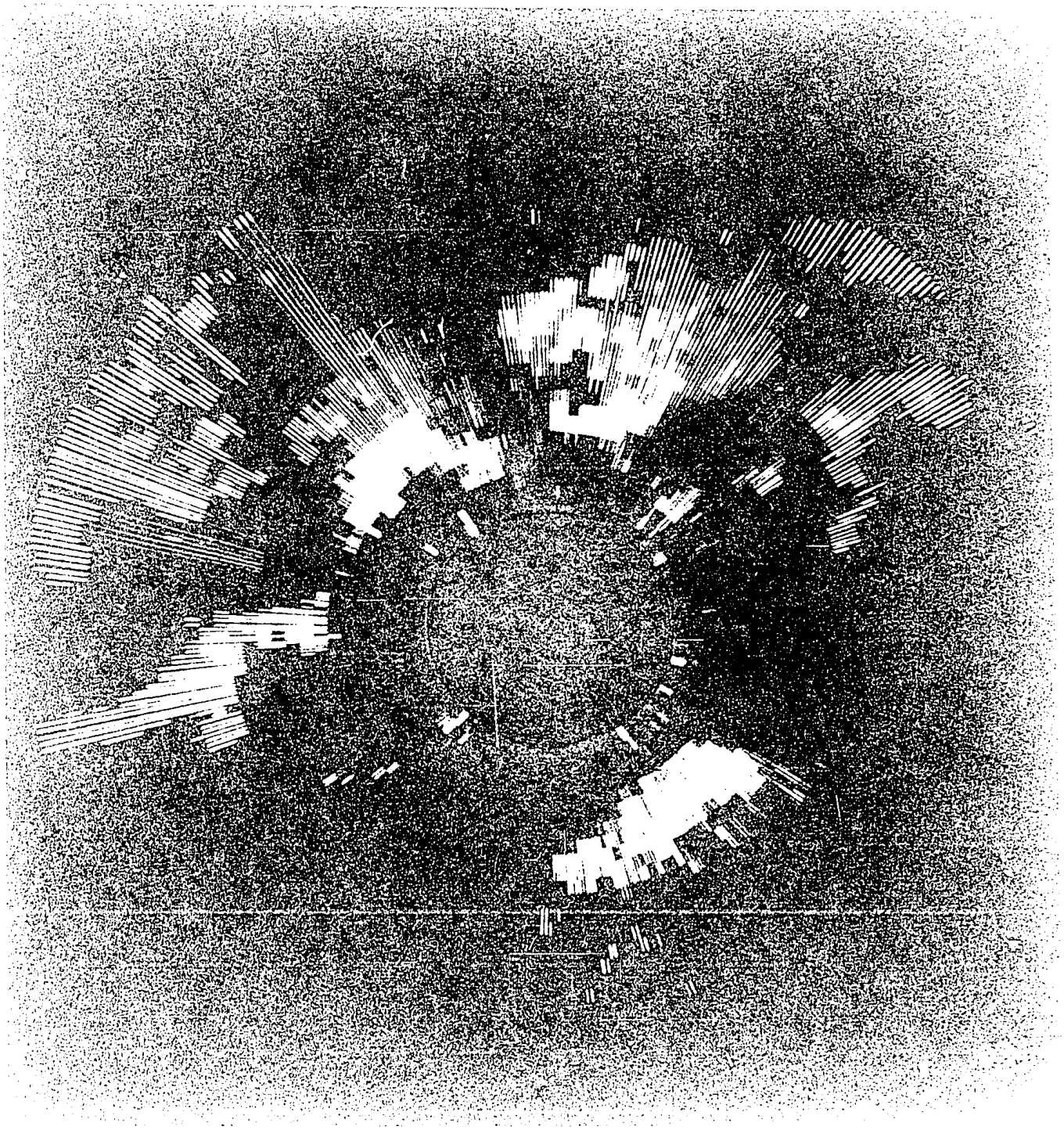

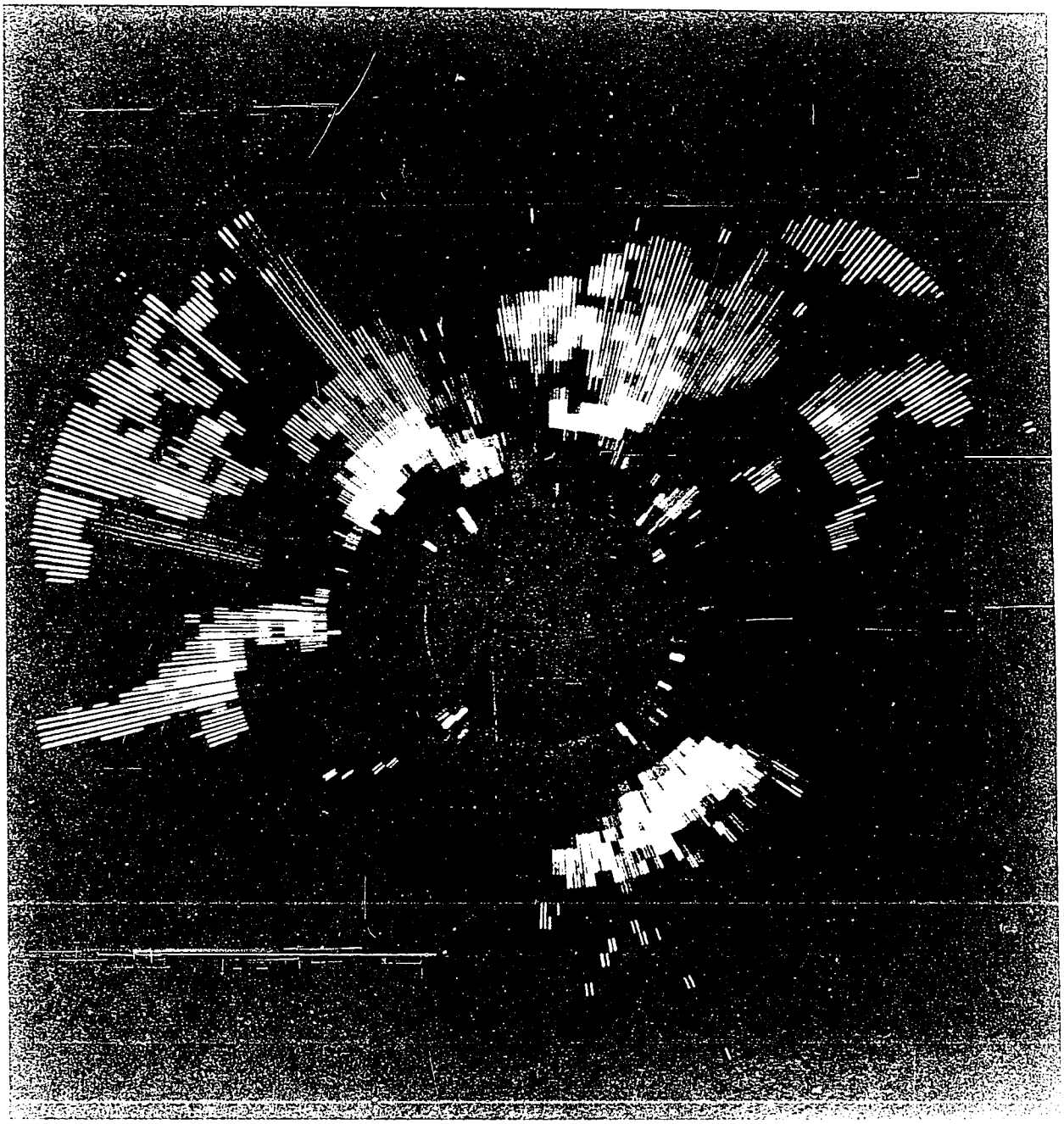

## 6. The Integrator

The use of stepped grey scale in any weather radar display, whether HARPI or CAPPI or PPI or RHI, is more effective if the data from several pulse lengths in range are integrated, and if the data for that range from several successive pulses are combined. This is performed by the Integrator by finding the maximum signal within the specified interval (several pulse lengths long), and 8 successive pulses, and displaying it as a constant signal for the same length of interval in time or range.

Averaging over 8 successive pulses, with 480 sweeps per second going into the Integrator, results in just 60 per second coming out. Any picture written with a sweep rate of 60 $sec^{-1}$ avoids certain patterns that otherwise tend to appear because of the residual 60-Hz field around the cathode ray tube.

During an experimental stage, the Integrator was used to produce PPI pictures. One such is presented in Fig. 8. Thirty range intervals, 2 nmi each, are present, from the minimum range 20 nmi to maximum 80 nmi. The integration was performed over two miles and 4 pulses (during the fifth pulse the integrated video was displayed on a CRT). The radar PRF was 186 Hz and therefore the read-out frequency was only 37.2 Hz. The antenna rotation period was 12 sec which with the above frequency represents approximately one radial line per degree of azimuth. This explains the spoked pattern of the picture.

The output of the Integrator was quantized in steps of 10 db, which are represented by steps in the shades of grey. The boundaries between shades are very well defined as a result of the integration. This picture represents an important improvement in the display of weather data which may justify the addition of an Integrator to many conventional radar displays.

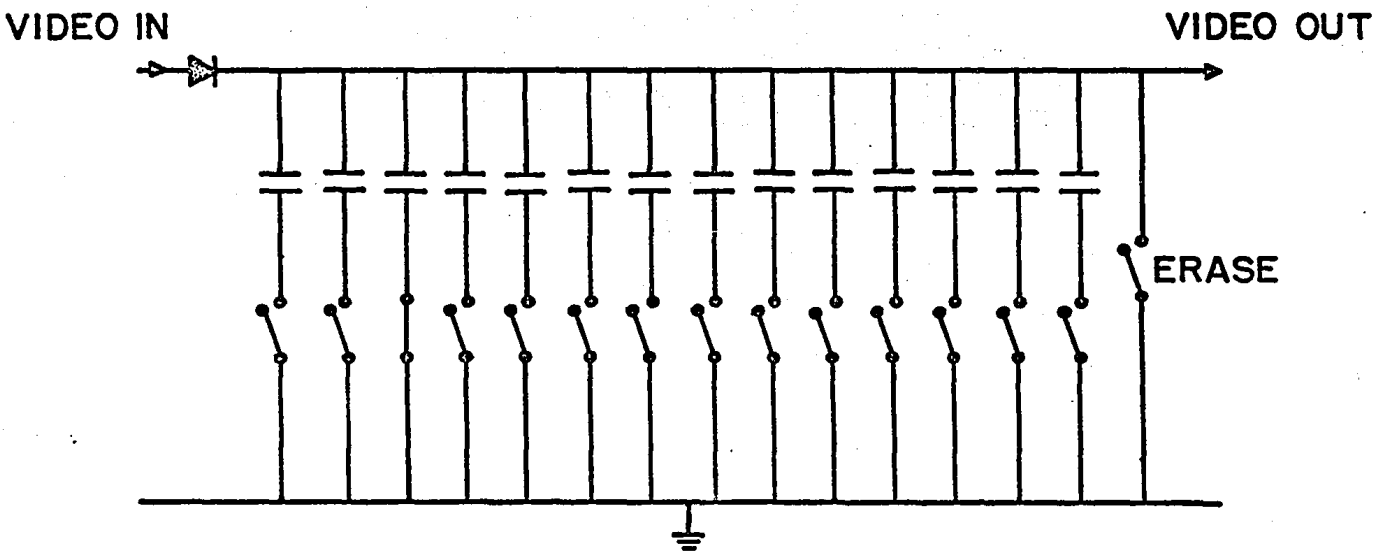


FIG. 9

The Integrator is an analog peak reader consisting of 14 storage capacitors corresponding to as many range intervals (Fig. 9). Each capacitor is connected at one terminal to a switching transistor turned on and off by an appropriately timed gate. The other terminal is connected to the input of the video signal through a diode. During the conducting state of a single transistor switch (third in Fig. 9) all others are off, therefore only one capacitor is charged at a time. The voltage across the capacitor follows the video signal as it rises and stays at its maximum value. The duration of the gate sets the range interval over which the peak reading is performed. After all the capacitors have been connected to the video in turn, each holds the maximum reading in one of the 14 range intervals.

The next pulse starts the process again and the voltage across the capacitors is altered only if the new signal exceeds the preceding. In this way the integration is extended over 8 pulses. With a PRF of 480 Hz the complete integration cycle lasts 1/60 sec. After that time the value which is read out is the maximum video signal in the chosen range interval, in 1/60 sec and in 0.8 degrees in azimuth (for an antenna rotation rate of 8 rev $min^{-1}$).

A switching transistor across the terminals of the capacitors is turned on after the information has been read out, acting as a discharge path or erase. When the ninth pulse appears the Integrator is ready for a new charging cycle.

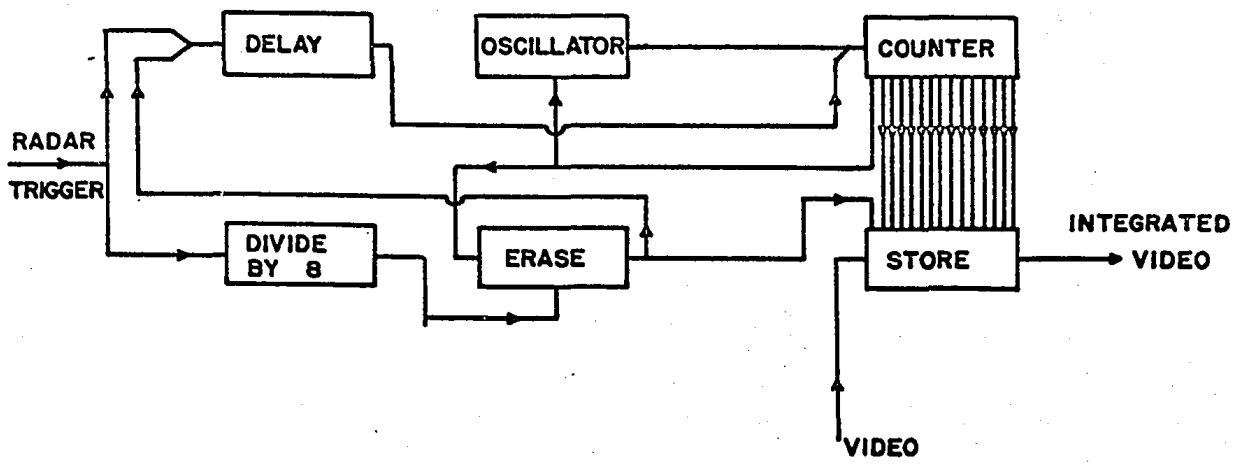


FIG. 10 a

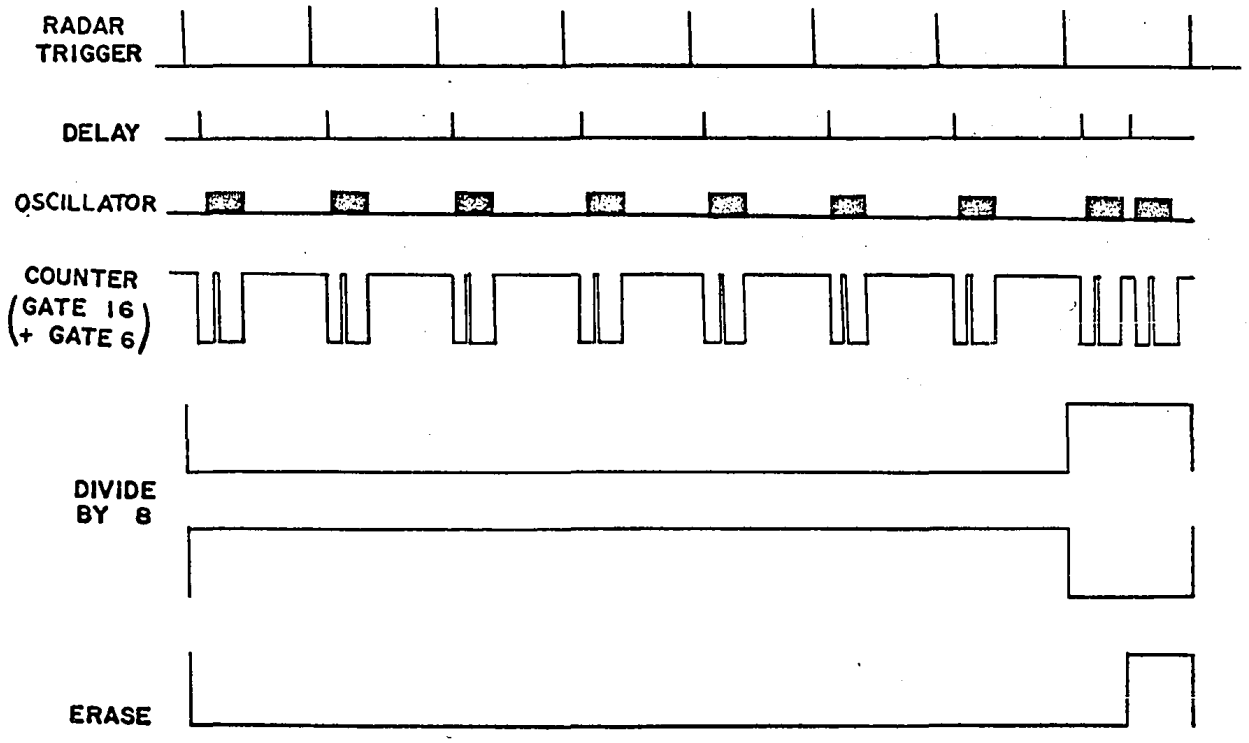


FIG. 10 b

Fig. 10a is a block diagram of the Integrator and Fig. 10b shows the waveforms at the outputs of some of the units. The function of the Delay (Appendix 2) is to produce a pulse delayed from the radar trigger which thereafter is used to start the operation of the system. Therefore it sets the minimum range at which the integration begins. The Oscillator and Counter (Appendices 3 and 5) perform together: the Oscillator provides triggers to the Counter, which in turn inhibits the Oscillator after all the Integrator switches have been activated. The period of oscillation sets the range intervals and is adjustable to two values: 25.2 $\mu$sec (2 nmi) and 63 $\mu$sec (5 nmi).

The Counter produces 16 individual gating waveforms, each from a separate terminal. The first is not used, the next 14 operate the switching transistors, and the 16th is fed back to the Oscillator to halt its action. Thus the Oscillator-Counter is self-inhibited after 16 oscillations. To initiate its operation again an external pulse to the Counter is needed in order to remove the inhibiting gate. This is provided by the Delay after a transmitter trigger, and in this way the oscillation is initiated again. Therefore a burst of 15 pulses is produced by the Oscillator after every delayed trigger. The reason for not using the first gate is that it is produced independently from the Oscillator (by the Delay) and requires a separate adjustment. The duration of this gate adds to the minimum range delay, the total of which is adjustable from 10 nmi to 35 nmi in 5 nmi steps. In Fig. 10b a typical gate (No. 6), and the 16th gate, are shown. In order to complete the integration cycle, the Store (Appendix 6) has to be read out and erased after the 8th pulse.

An FET source-follower is used to read out the voltage across the capacitors when the switches are closed for the eighth time. The high impedance presented by this circuit element ensures a minimum loss of charge during the preceding seven switching operations. The Erase flip-flop is triggered by the 16th gate. During the first 7 pulses it is held off by the Divide-by-8 (Appendix 7); after the 8th the Divide-by-8 releases the flip-flop, allowing it to be triggered by the 16th pulse. The Erase gate (Appendix 8) closes the discharge switch and simultaneously triggers the Delay. The action of the Oscillator is initiated and each capacitor is connected to the discharge path. The integrated video output is quantized by a Threshold Amplifier (Appendix 9) in 7 steps, each corresponding to a 10-db change in received power. These are adjustable to any other value, or for the purpose of calibration.

In describing the action of the peak reader, ideal behaviour of the components was assumed. Actually the finite impedance of the charging path prevents the voltage across the capacitors from following the video signal exactly. An emitter follower at the input reduces the time constant of the charging circuit to such a value that a signal lasting 1 $\mu$sec charges the capacitor to 90% of its amplitude.

On the other hand the amount of leakage from the capacitors depends on the number of times the switches are operated. The fact that both the charging time and the loss through leakage are finite implies that some degree of averaging of the echoes is performed. With a high-PRF radar, the echoes from two consecutive pulses are not independent and the two

signals differ only by a small amount. Therefore the second pulse reduces the effect of the finite charging time.

A direct comparison of video signal and integrated output can be used to evaluate the extent to which the echoes are averaged. Fig. 11 is an oscillogram showing the video signal produced by a storm at the input to the Integrator (lower trace) together with the corresponding output (upper trace). The video input trace is the result of 4 pulses superimposed (the radar PRF was 186 Hz). Comparisons of input and output, from many such pictures, show that the Integrator is a peak reader within approximately 1 db, and therefore the amount of averaging is in practice negligible.

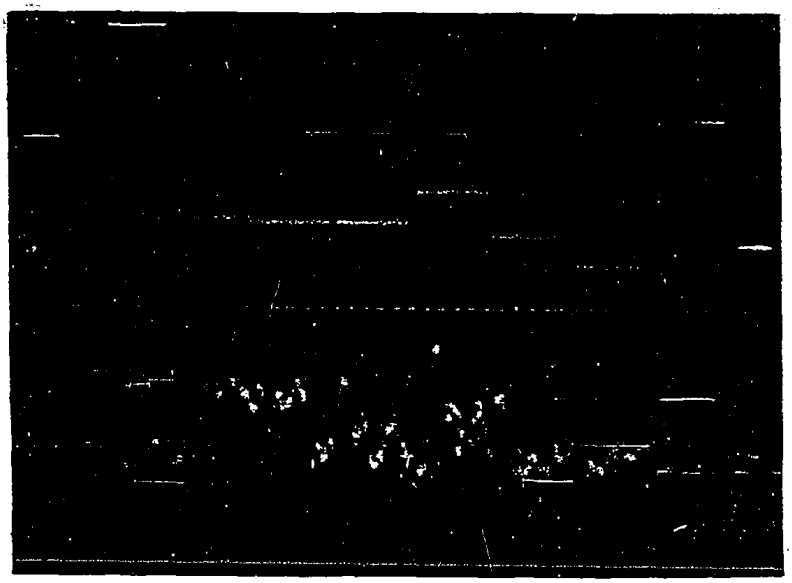

FIG. 11

signals differ only by a small amount. Therefore the second pulse reduces the effect of the finite charging time.

A direct comparison of video signal and integrated output can be used to evaluate the extent to which the echoes are averaged. Fig. 11 is an oscillogram showing the video signal produced by a storm at the input to the Integrator (lower trace) together with the corresponding output (upper trace). The video input trace is the result of 4 pulses superimposed (the radar PRF was 186 Hz). Comparisons of input and output, from many such pictures, show that the Integrator is a peak reader within approximately 1 db, and therefore the amount of averaging is in practice negligible.

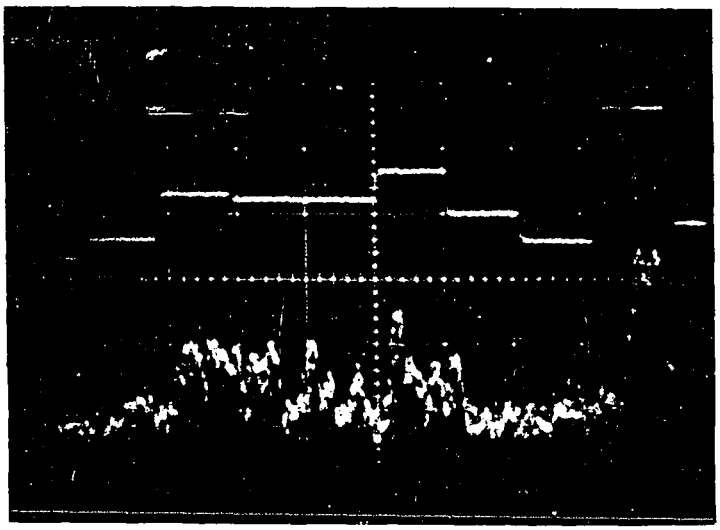

FIG. 11

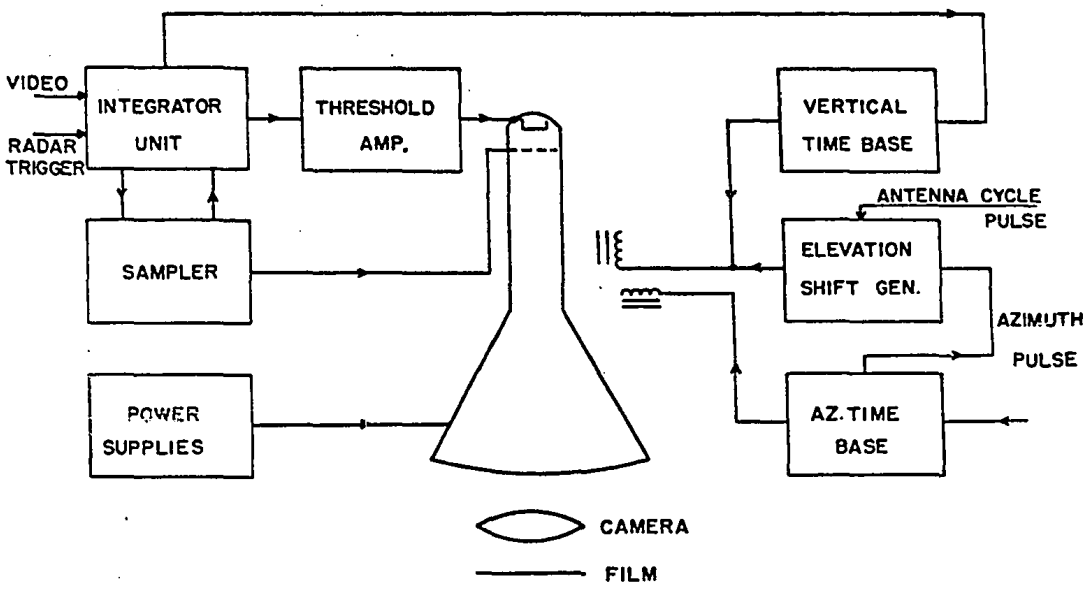


FIG. 12

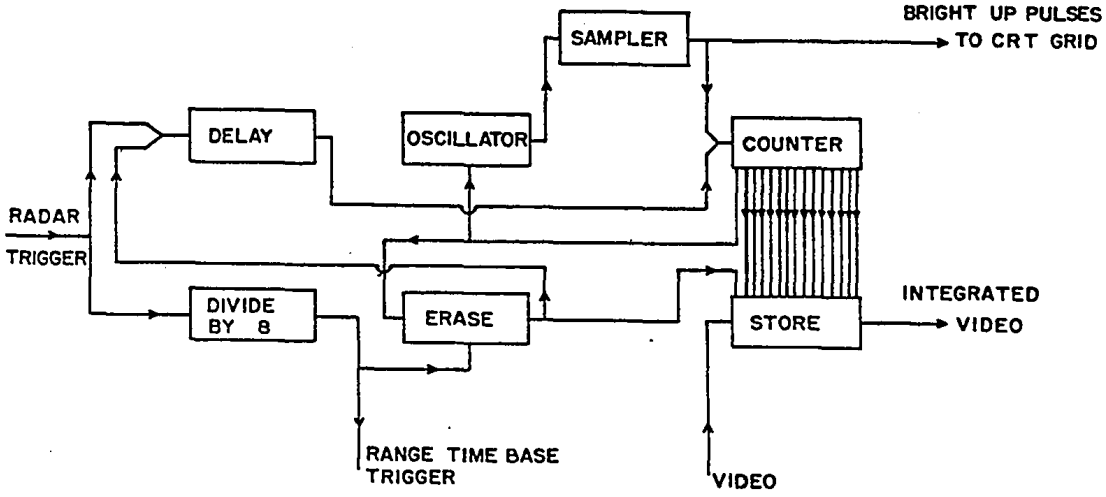


FIG. 13a

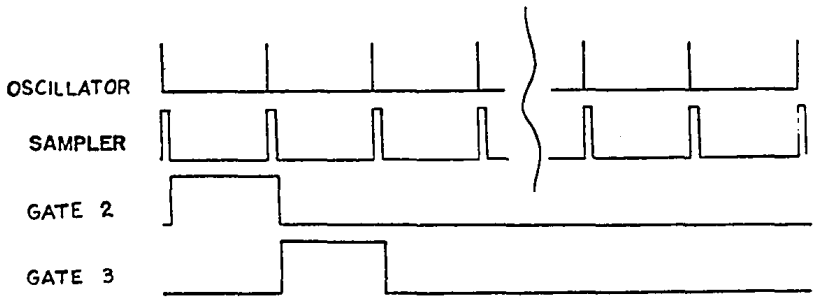


FIG. 13b

## 7. HARPI Circuitry

Fig. 12 is a block diagram of the HARPI display. The integrated video, quantized by the Threshold Amplifier, is applied to the cathode of a high resolution CRT. Two time bases deflect the electron beam in rectangular coordinates. In the X-direction the time base is slow, corresponding to the rotation of the antenna, being thus the azimuth axis. A linear sweep in the Y-direction is started every 8th or Integrator read-out pulse to represent range. These alone would yield the well-known B presentation.

When the Integrator is used with the HARPI display, a modification is introduced (see Fig. 13a, which should be compared with Fig. 10a): the Oscillator triggers an additional monostable (Sampler in Fig. 13a) which produces pulses of length equal to 1/20 of the oscillation period, and the trailing edges of these trigger the Counter. The effect of this arrangement is that the Sampler pulses occur at the end of every gate. The waveforms in Fig. 13b illustrate this. The Sampler is described in detail in Appendix 4.

The output of the Sampler monostable is applied to the grid of the CRT which normally is biased off. Only at the time of a pulse from the Sampler does the screen brighten up with an intensity proportional to the Integrator output. Therefore only 1/20 of every range interval is displayed by a single time trace. It should be remembered that the integration assigns a single value for the entire range interval, so that there is no loss of information due to this sampling process. After the first rotation of the antenna there are 14 lines displayed on the CRT, separated by a space equal to 20 times their width (instead of the B

presentation), each containing all the information from one range interval. Since this display of the sampled video occurs after the 8th transmitter pulse, the read-out is simultaneous with the last video signal contributing to the integration. However, there is no need to cut off the input video during the read-out because the sampling pulse is at the end of each gate.

After every complete rotation of the antenna the origin of the range trace is shifted along the range axis. The displacement is equal to the width of the sampling pulse, and is produced by a staircase voltage of 20 steps added to the Y deflection and produced by the Elevation Shift Generator (Appendix 10). In this way, the information from each antenna rotation is placed above the preceding one. A spiral antenna programme consisting of 20 rotations will fill the space between range intervals with height information, and a film exposed during the entire antenna cycle will compose the HARPI presentation.

Although the data processing and the integration are done together in this system, the Integrator could be used independently. The film acts simultaneously as a storage element during the composition of the presentation and as a recording medium. Polaroid film type 107 was used during the evaluation period.

8. Range resolution of the display

The division of space into discrete elements, together with the presentation of maxima of received signals, creates new problems regarding resolution and accuracy of the display. The integration is performed in azimuth over 0.8 degrees which is less than the beam-width, and therefore the limits of resolution are set by the beam-width and not by the display. In the vertical dimension the limitation in resolution is set by the antenna program. For range resolution, the integration over 2 nmi degrades the capability of this particular radar by a factor 15. Three questions are of interest: 1) given a single prominent echo in a background of lower intensity, what is the uncertainty in its size L, and in its position in range? 2) given two such features, what must be their separation in order to appear in different HARPI sections? and 3) what should be their separation in order that they be distinguishable as two individual features rather than two parts of a single larger feature (that is, appearing in two HARPI sections separated by a third).

The answers to these questions are statistical in origin and thus the notion of probability will be involved. If the extension in range of the single feature is L = 2 nmi, it is unlikely that its position with respect to the radar will be such that it will appear in only one HARPI section. On the other hand, if L is (say) 0.1 nmi, this likelihood is considerably increased. Assuming (1) that all positions with respect to the radar are equally probable and (2) that all the values of L are equally probable, we can formulate the above considerations in quantitative form by observing that if an echo appears in precisely one HARPI section then the probability P(L,dL) that the range extension will fall between L and L + dL will be proportional to the space inside which the feature

can be located, that is to the difference between the range interval ($\Delta r$) and extension in range (L). Thus we have

$$PdP = K(\Delta r - L)\, dL \qquad (8)$$

where K is a constant in proportionality.

The normalization condition may be written:

$$\int_0^{\Delta r} PdP = 1 \qquad (9)$$

The upper limit of this integral represents the condition that the feature appears in only one HARPI section.

Substituting PdP from equation (8):

$$K \int_0^{\Delta r} (\Delta r - L)\, dL = K\Delta r \int_0^{\Delta r} dL - K \int_0^{\Delta r} L\, dL$$

then $$\frac{1}{K} = \Delta r^2 - \frac{\Delta r^2}{2} = \frac{\Delta r^2}{2} \quad \text{and} \quad K = \frac{2}{\Delta r^2}$$

Therefore $$PdP = \frac{2}{\Delta r^2} (\Delta r - L)\, dL \qquad (10)$$

If the feature appears in precisely two HARPI sections it is convenient to distinguish two cases: a) $L > \Delta r$ b) $L < \Delta r$. In case a) the same procedure is valid as for the case of one single HARPI containing the feature but with twice the range interval as before:

$$PdP = K_1 (2\Delta r - L)\, dL \qquad (11)$$

In case b) the density of probability is proportional to L:

$$PdP = K_2 L\, dL \qquad (12)$$

For $L = \Delta r$ both expressions have to be equal and therefore

$$K_1 = K_2 = K$$

Normalizing simultaneously the expressions (11) and (12):

$$K\left[\int_{\Delta r}^{2\Delta r} (2\Delta r - L)\, dL + \int_{o}^{\Delta r} L\, dL\right] = 1$$

$$2K\left(\tfrac{1}{2}\Delta r^2\right) = 1 \qquad K = \frac{1}{\Delta r^2}$$

Therefore in the case of a feature extending into two HARPI sections:

$$PdP = \begin{cases} \dfrac{1}{\Delta r^2}\,(2\Delta r - L)\, dL & \text{if} \quad \Delta r \leqslant L \leqslant 2\Delta r \\ \dfrac{L}{\Delta r^2}\, dL & \text{if} \quad 0 \leqslant L \leqslant \Delta r \end{cases} \tag{13}$$

This expression has a maximum at $L = \Delta r$ and is symmetrical about it.

The extension to the case when the feature appears in a number ( J ) of HARPI sections with $J > 2$ follows similarly:

$$PdP = \begin{cases} \dfrac{[L - \Delta r(J-2)]dL}{\Delta r^2} & \text{if} \quad \Delta r(J-2) \leqslant L \leqslant \Delta r(J-1) \\ \dfrac{(J\Delta r - L)}{\Delta r^2} & \text{if} \quad \Delta r(J-1) \leqslant L \leqslant J\Delta r \end{cases} \tag{14}$$

which is always symmetrical with a maximum probability of finding L equal to $\Delta r(J - 1)$.

From the foregoing, after examination of a HARPI picture, it is possible to find a value $L_o$ which is the best estimate of the extent of an actual feature. This value is the value of L which divides the area under the appropriate probability curve into two equal parts. In fifty per cent of the cases the feature will extend in range more than $L_o$ and in fifty per cent of the cases will extend less than $L_o$, but in average (over many independent measurements) $L_o$ will be a good approximation to the average extension in range of the echoes appearing in a given number (J) of adjacent HARPI sections. In the case of expression (14) the maximum likelihood estimate of L is given by

$$L_o = \Delta r \, (J - 1) \tag{15}$$

which coincides with the value at which the probability (P) is maximum.

In the case of expression (10) the value of $L_o$ is found by writing

$$\int_o^{L_o} PdP = \tfrac{1}{2} = \frac{2}{\Delta r} \int_o^{L_o} (\Delta r - L)\, dL$$

The solution of this equation is:

$$L_o = 0.3 \, \Delta r \tag{15'}$$

and for $\Delta r = 2$ nmi gives the value $L_o \approx 0.6$ nmi. With $\Delta r = 2$ nmi the uncertainty in position of echoes of size $L_o$ is 2 nmi in the case of expression (14) and 1.4 nmi in the case of expression (10).

Thus far it has been assumed that all echo sizes are equally probable. If there is an "a priori" probability with relation to sizes, the expressions (10) and (14) should be weighted accordingly, and normalized. Taking advantage of the fact that the resolution of a HARPI picture in azimuth is much better than that in range, and specially so at short ranges, it is possible to investigate this "a priori" probability by measuring the frequency distribution of sizes in azimuth.

The previous theory is qualified by the implicit assumption that the prominent feature which appears in one or more HARPI sections is produced by a single (continuous) target. If the possibility of discontinuities is considered the mathematics involved is more complicated, and although the form of expressions (10) and (14) change the values of $L_o$ remain unchanged.

On page 10 the advantages of displaying the maximum instead of the average in each range interval were discussed, and it was noted that the average can be estimated from the display. The use of $L_o$ makes this possible because it gives an estimate of the extent of any selected echo intensity. Having determined the extent of an echo observed in a certain group of adjacent range intervals, the average intensity is found assuming that the remainder of the space in the fringe range intervals is either of the next lower threshold of intensity or of zero intensity.

If the distance $\underline{d}$ between two prominent features is greater than 2 nmi then they will appear in separate HARPI sections. The range of possible positions with respect to the radar, such that the two features appear in separate HARPI sections, varies linearly with $\underline{d}$ when $d < 2$ nmi. On this basis we can express the probability (P) of finding the two features in two adjacent HARPI sections as:

$$P = \begin{cases} \frac{d}{2} & \text{if} \quad 0 \leqslant d \leqslant 2 \text{ nmi} \\ 1 & \text{if} \quad d \geqslant 2 \text{ nmi} \end{cases} \tag{16}$$

In order to be presented in two non-adjacent HARPI sections the distance between the two features must be at least 2 nmi greater than in the previous case. The probability of such an occurrence is:

$$P = \begin{cases} 0 & \text{if} \quad 0 \leq d \leq 2 \text{ nmi} \\ \left(\frac{d}{2} - 1\right) & \text{if} \quad 2 \leq d \leq 4 \text{ nmi} \\ 1 & \text{if} \quad d \geq 4 \text{ nmi} \end{cases} \qquad (17)$$

Thus two features will always be distinguished from a single larger one if the separation between them is $2\Delta r$ (4 nmi in this case). However, if the separation is $\sim 3.5$ nmi the two features will appear in non-adjacent HARPI sections in fifty per cent of the cases.

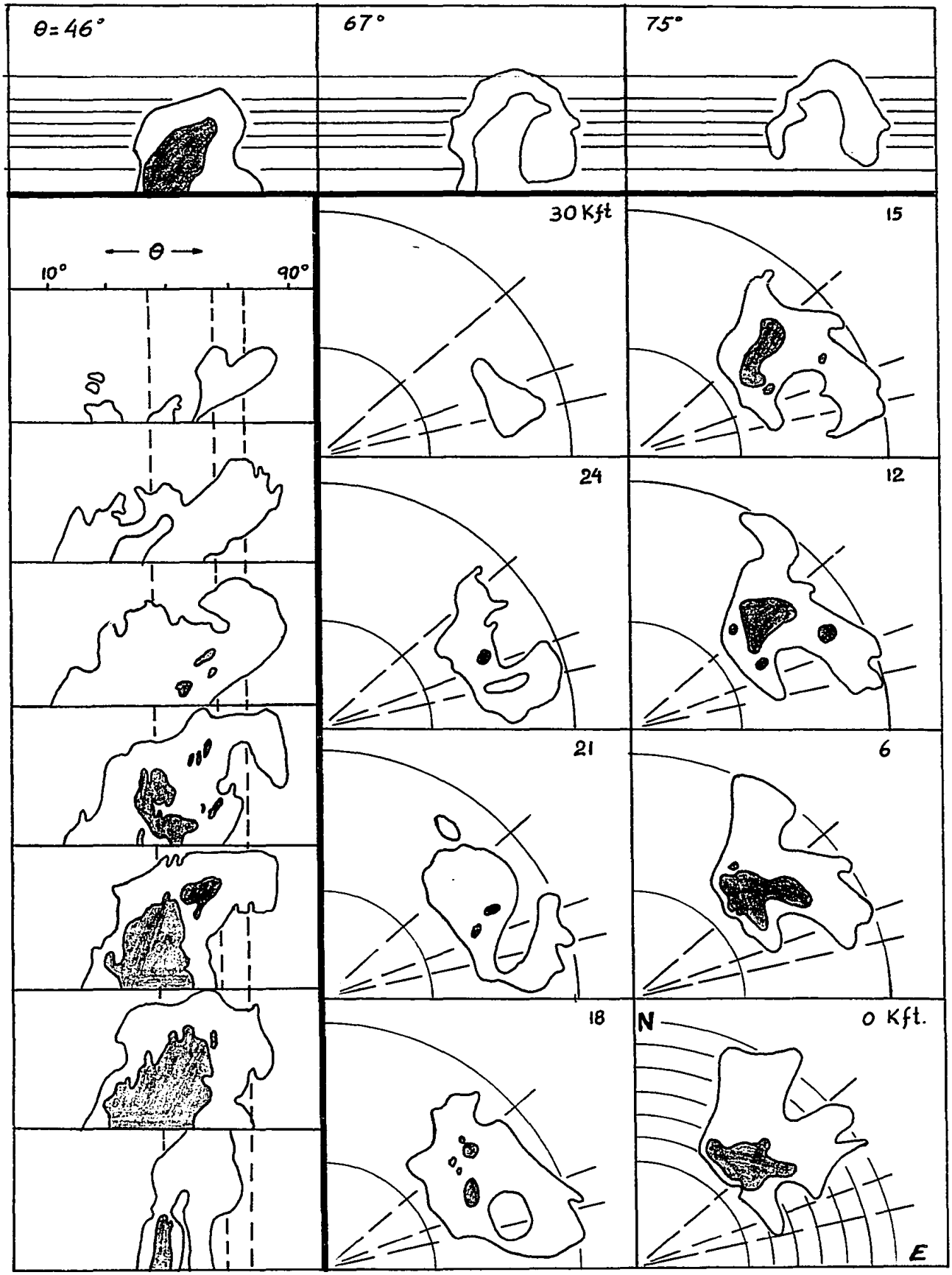


FIG. 14

9. Description of the storm of 28 July 67 at 1706-1709

The set of HARPI sections of Figure 7 shows an instant in the life of a storm described in space and intensity. A study of the structure of this storm has been prepared (see Figure 14). On the left-hand side of Figure 14 the HARPI sections have been redrawn (for simplicity only shades 1 and 3 are shown, although shades 2 and 4 are also available in the HARPI's). The top of this figure contains three RHI sections corresponding to azimuths indicated by the vertical dashed lines on the HARPI sections. The two columns on the right-hand side contain eight CAPPI levels with the heights stated. The lowest CAPPI map is the zero-degree PPI section with the position of the HARPI sections indicated by the circles and the positions of the RHI sections by the dashed radial lines. The rest of the CAPPI maps have indicated on them the extreme HARPI ranges and the RHI bearings. The CAPPI heights are indicated on the RHI sections by the horizontal lines. The RHI and CAPPI sections are hand-produced from the HARPI's, and smoothed from the discrete 2 nmi steps.

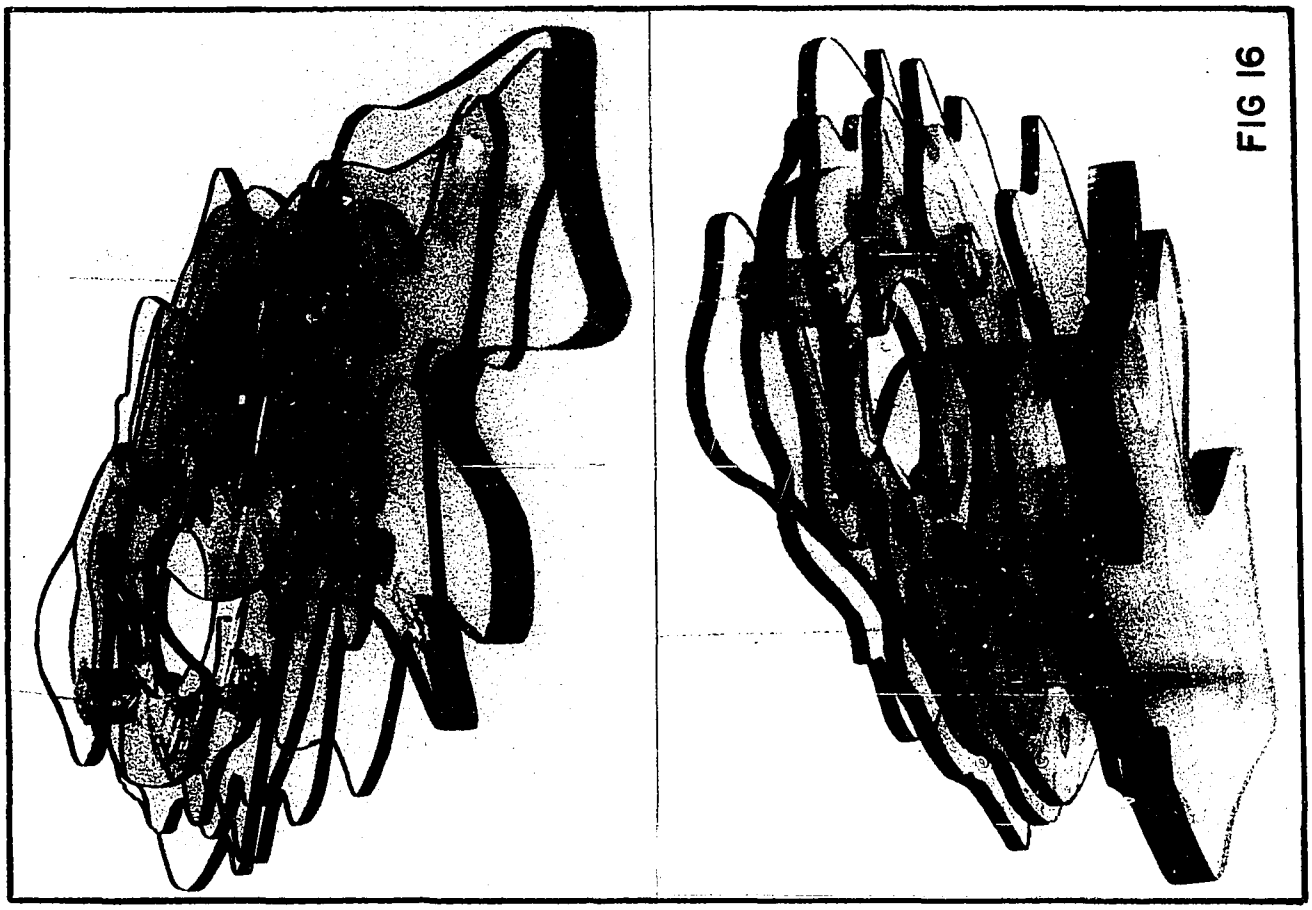

FIG 16

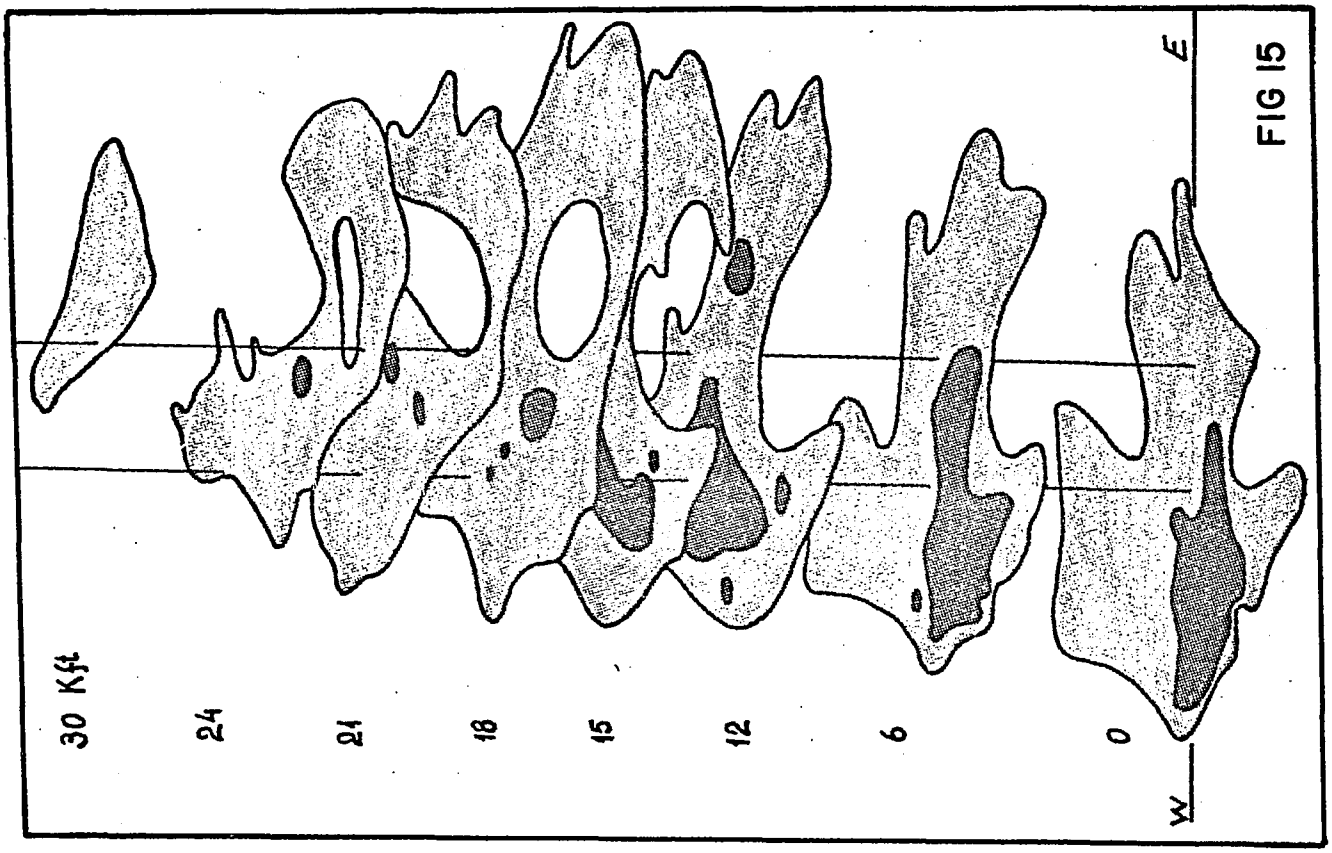


FIG 15

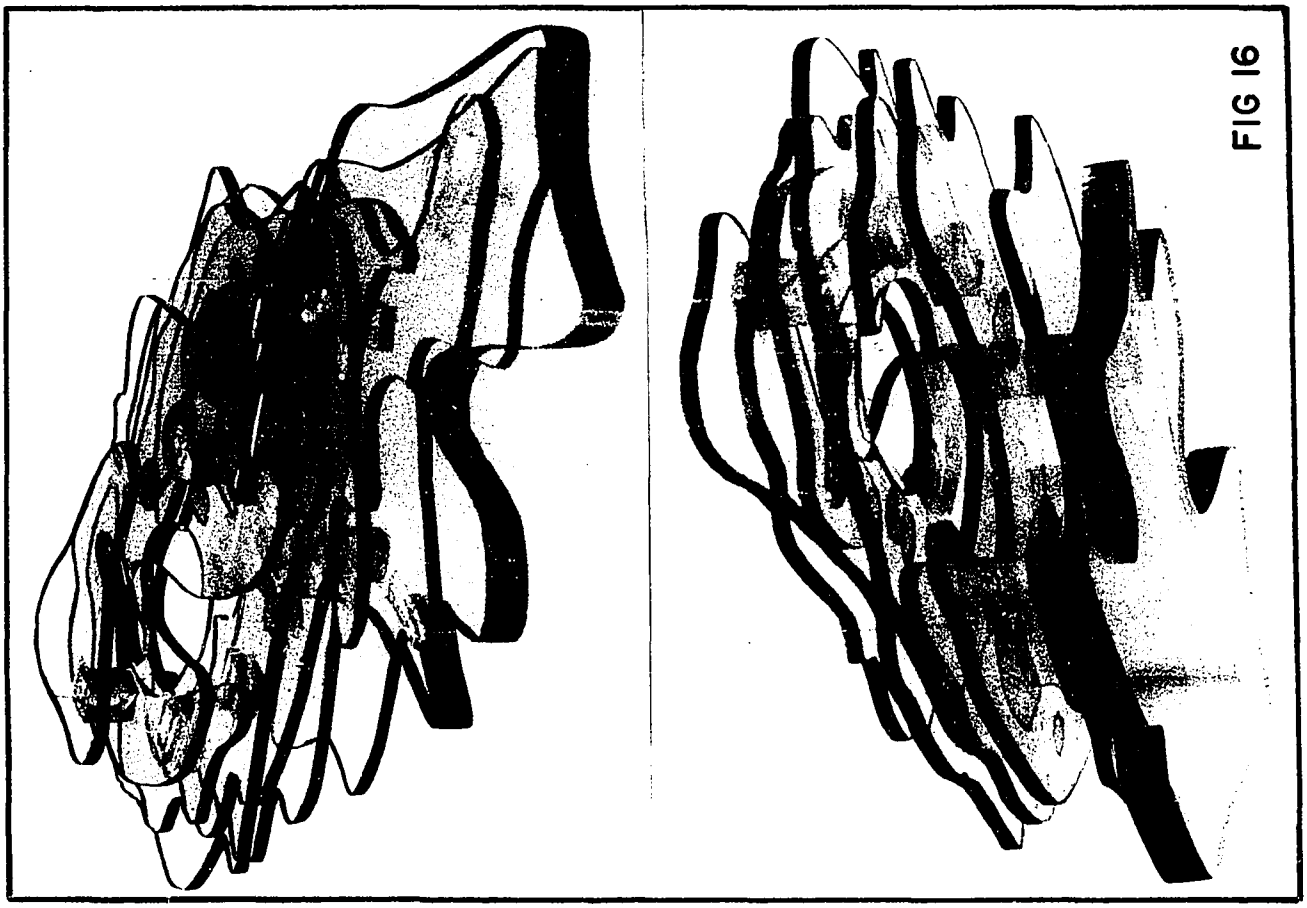

FIG 16

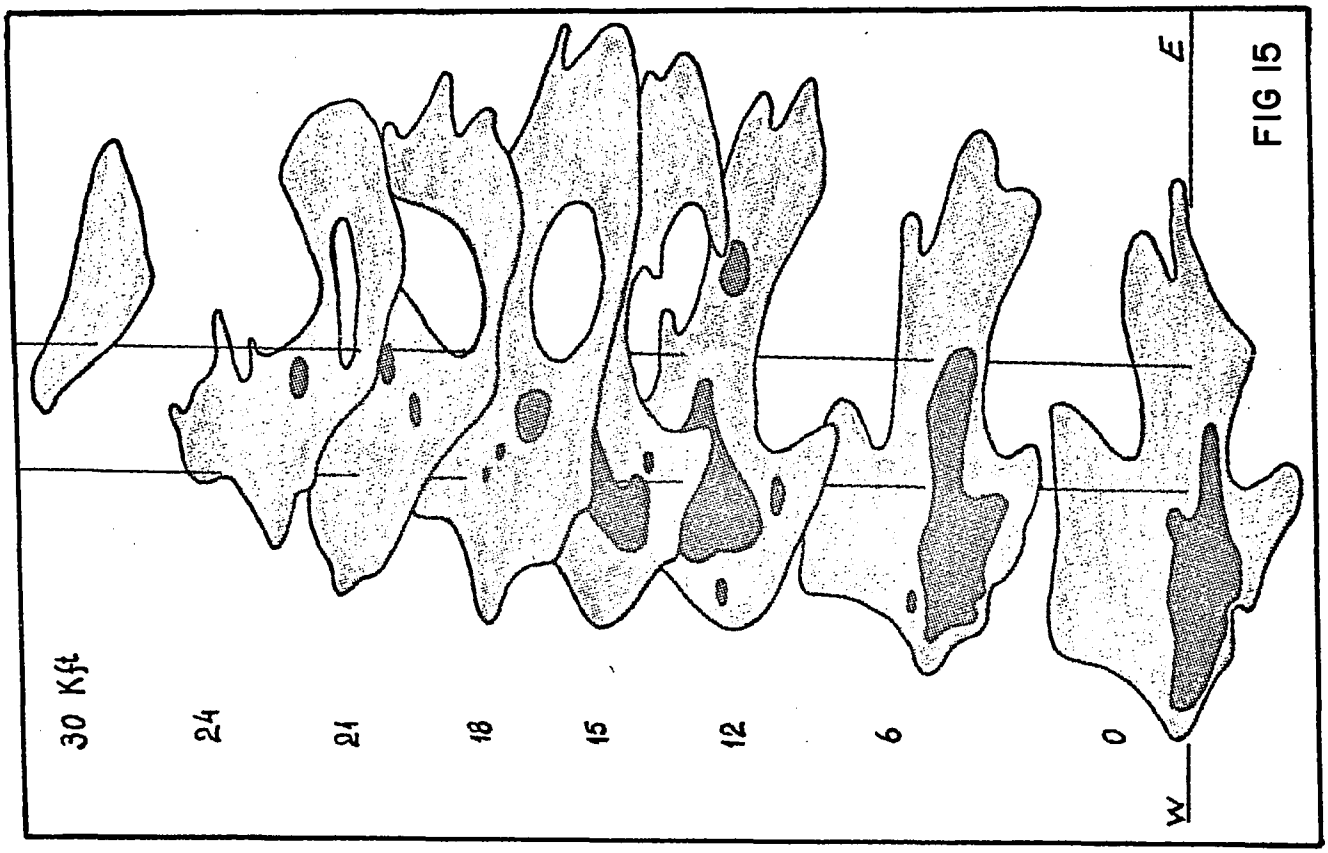


FIG 15

Two 3-dimensional models were made by assembling the CAPPI layers one above the other. In Fig. 15 the CAPPI maps have been drawn in perspective and spaced in order to give a vertical to horizontal scale ratio of 5:1. In Fig. 16 two photographs of a plastic model of the CAPPI maps assembled in a 1:1 scale are shown. The lower photograph was taken from below the model and the other from above and on the opposite side. The dotted zones correspond to shade 3.

The last three figures (14, 15 and 16) enable a clear interpretation of the geometry of the storm. From Figure 15 the storm appears to slope eastwards with sharp gradients of intensities toward the radar site and an echo-free region to the south-east (the most intriguing feature). This region which penetrates inside the storm more and more with increasing height, forms a hole at 18 kft and then turns abruptly in a direction normal to its original major axis as it comes out of the storm. Two vertical lines have been added to Figure 15 to reveal the sloping of (1) the region of high water content(shade 3) and (2) the echo-free region. The latter region slopes towards the east and less markedly toward the north. The lower photograph of Figure 16 shows the entrance to the echo-free region of the storm. The top photograph shows the exit from this region at high altitudes. One can observe the sharp change in direction between 12 and 24 kft as compared with the first 12 kft. The elongated hole at 24 kft appears to be an overshoot of the echo-free region. It is seen in Figure 5 that this region is a characteristic present in the structure of the storm during most of its life-cycle and is possibly related to the mechanism of evolution of this particular type of convective thunderstorm.

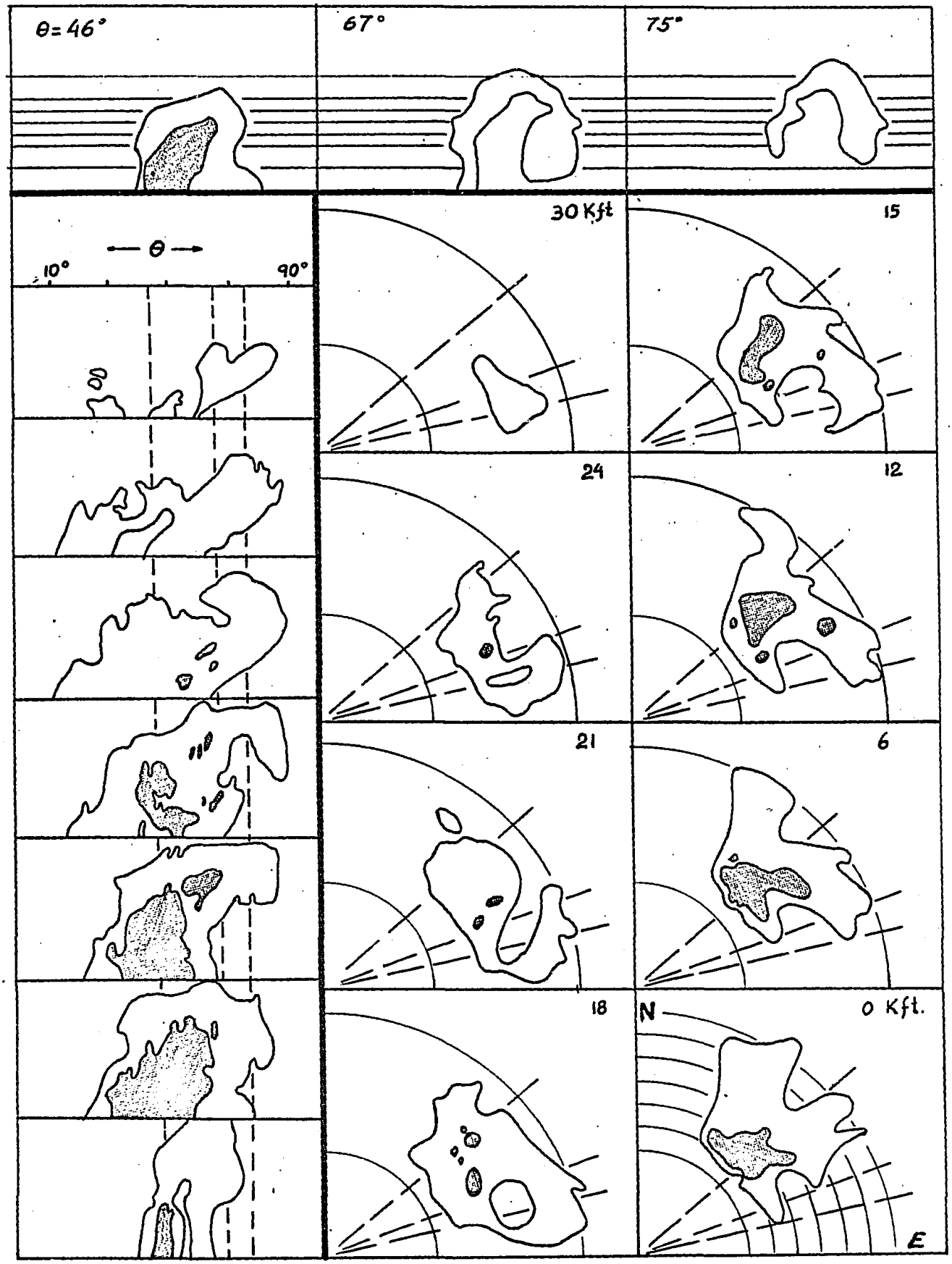


FIG. 14

The CAPPI maps in Figure 14 also show the degree of penetration of the echo-free region with height. Its major axis is seen to rotate from a NW-SE to a NE-SW direction and the intense precipitation is shown tending to surround the echo-free region with a similar rotation of its major axis. This suggests a inter-relation between the two zones of the storm. The sloping with respect to the vertical of these regions is not apparent on the CAPPI maps, but is clearly presented by the RHI sections.

On the HARPI sections the display of the maximum instead of the average of the signal produces a picture where the extension of the echo is overestimated while the echo-free region underestimated. This has to be borne in mind and a mental compensation made when the pictures are observed. Considering now the HARPI's in Figure 14 it is seen that in the third section (14-16 nmi) the eastern part of the storm (right-hand side of the section) is narrower at low levels than either the preceding or the following section, leaving therefore a concavity in the echo at 14-16 nmi. At higher levels the echo-free region is at 16-18 nmi enclosed by the sections at 14-16 nmi and 18-20 nmi, thus the radial sloping is apparent. Finally there is an opening in this region at 18-20 nmi toward the northern part of the storm. The overhang at 16-18 nmi completely encloses the echo-free region which forms a hole inside the storm. The region of high water content (shade 3) tends to be predominate near the echo-free region. There is a pocket of shade 3 aloft at 14-16 nmi just to the left of the hole.

Observing HARPI's and RHI's together the echo-free region appears aloft surrounded by a "cap" of precipitation.

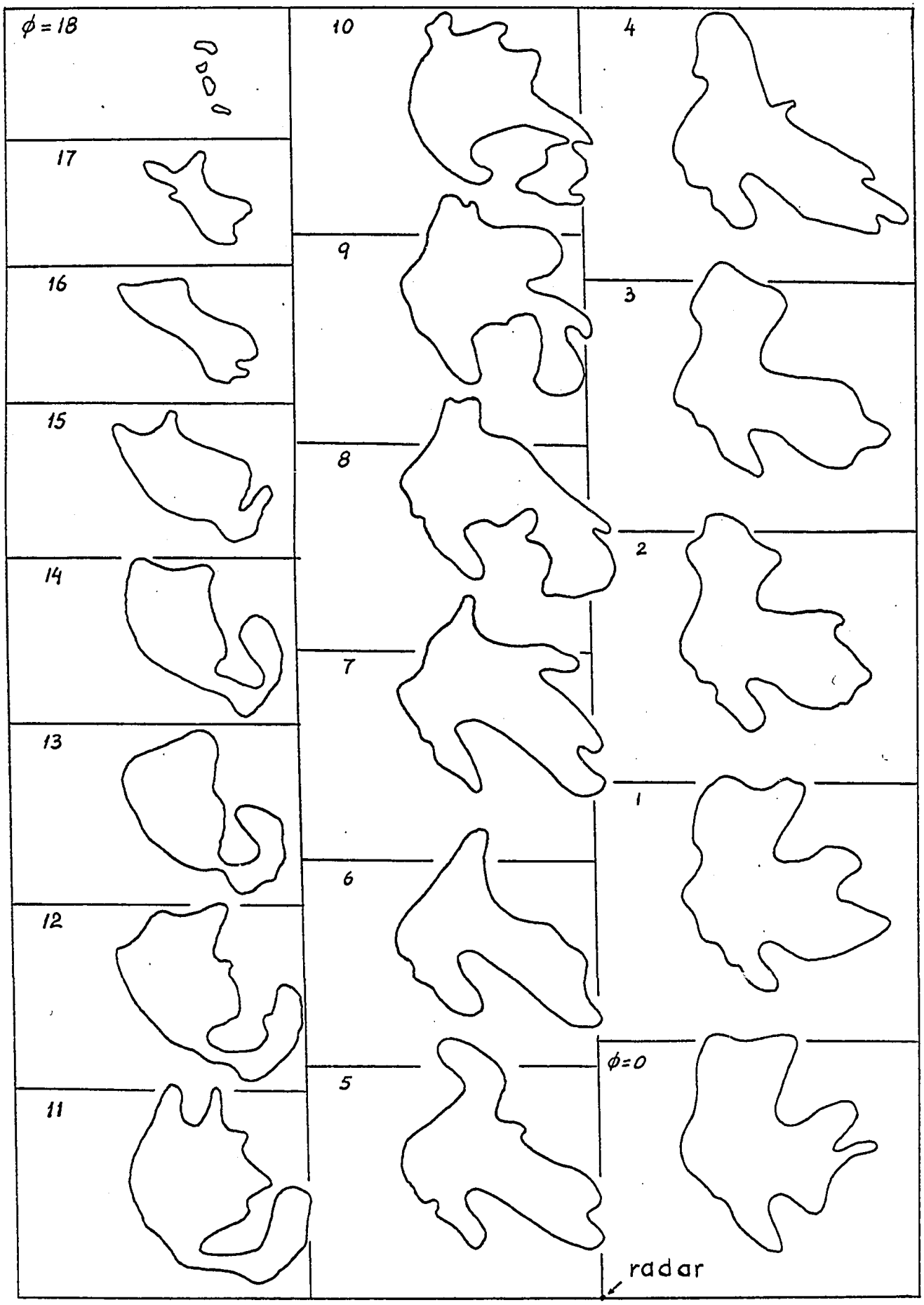


Figure 17 - PPI sections obtained from the HARPI sections of Figure 7

## 10. Evaluation of presentations of radar data

From the discussion of the previous chapter it appears that every type of section across the storm contributes to the understanding of the geometry of a storm. A single set of sections will give an incomplete picture, and even three perpendicular sections like those of Figure 14 are not as clear in some respects as a 3-dimensional model. Some such model generally would be extremely useful as a first step towards the analysis of a storm.

There follows below an evaluation of different presentations in relation to their ability to fulfil the two primary tasks: conveying 5-dimensional information and storing this information. Two presentations will be considered briefly first: the PPI, in use in Alberta, and the RHI. PPI's display conical sections, which in the region $r > 60$ nmi where the total height of the storm is scanned by some 5 beams ($1^{\circ}$ beamwidth), are a good approximation to CAPPI's. However, for shorter ranges where the antenna program gives very detailed information the PPI's give a distorted picture even for small storms (when the cone can be approximate by a sloping plane). In Figure 17 the set of 19 PPI sections corresponding to the same instant in the life of the storm as the CAPPI's of Figure 14 are shown. The idea about the shape of the storm emerging from these sections could be misleading. PPI presentation does not convey the 3-dimensional space in a true sense of the word and is useful only as a storage form. When the information has to be processed the first step is to transform the information in the form of CAPPI's, RHI's or HARPI's as experience shows.

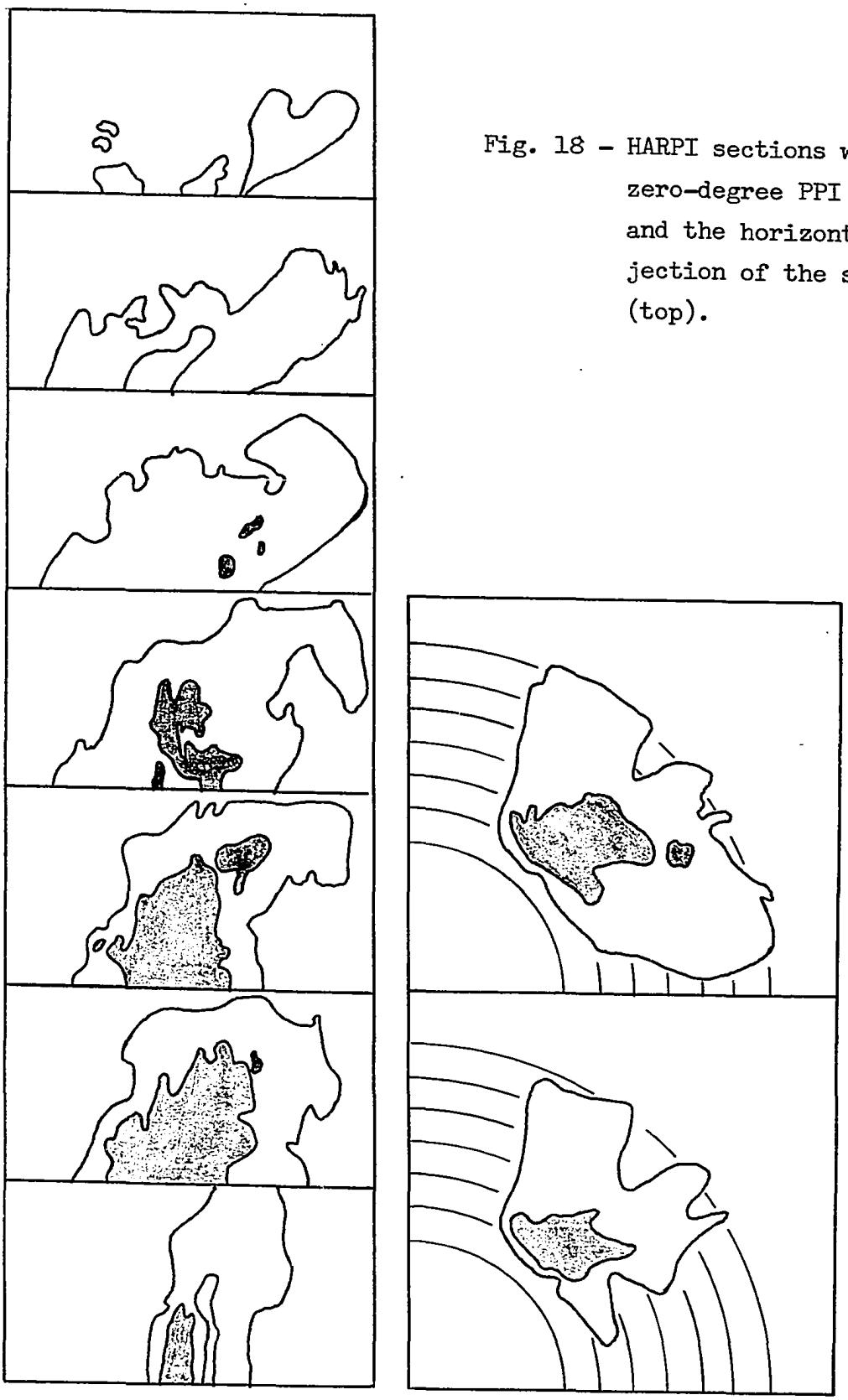

Fig. 18 - HARPI sections with the zero-degree PPI (bottom) and the horizontal projection of the storm (top).

The RHI presentation displays the vertical structure of the storm and therefore should be compared with HARPI. It should be noted first that the vertical scanning of the antenna which directly yields RHI's would produce too much strain on the mechanical elements of an antenna system such as the one used in Alberta. The weight of the antenna implies large accelerations if such a scanning program is to be used. Therefore the RHI sections would have to be produced by processing electronically obtained data with an antenna program such as the one described in chapter two. This is in some ways analogous to the HARPI system. The other consideration, which makes HARPI's decidedly more convenient is that, with a storm subtending say $60^{\circ}$ in azimuth there are needed 60 RHI sections to describe the storm with $1^{\circ}$ resolution. The reconstruction of the structure in space of the storm from such 60 sections is extremely difficult. RHI's are very useful to illustrate a limited sector of the storm but they are not convenient to represent the 3-dimensional space.

The presentations considered in detail will be the CAPPI and the HARPI. In addition, a combination of HARPI's and one map-type picture will be considered. Such a combination is shown in Figure 18 where the HARPI sections are shown together with the zero-degree PPI section (bottom) and a projection of the whole storm on the horizontal plane (total CAPPI). With either of them the storm can be reconstructed by placing the HARPI sections over the map-type presentation.

The evaluation will be made for storms which subtend not more than $90^{\circ}$ in azimuth. Such is the case of Alberta storms where even at short ranges of the order of 10 nmi this is valid. With $90^{\circ}$ subtended

the cylindrical section does not differ from a plane one, and this is the optimum situation for the HARPI display. For larger storms the analysis will be valid when small sectors are of interest, such as snow-generating cells in winter situations.

A relative comparison will be made using a scale of poor, satisfactory and good to consider the presentations with respect to the following characteristics:

a) Comprehensibility of presentations: This is the facility with which an observer can reconstruct in mind the internal structure of the storm from the cross-sections which compose the presentation.

CAPPI's give the best picture of the horizontal structure. In the vertical, however, they require imagination in seeing continuity between the levels.

HARPI's display well the vertical structure inside a slice of the storm. For the type of storms considered here the distortion due to the opening of the cylinders is negligible. When a feature is sloped radially it is split between two sections and requires mental connection, but this provides simultaneously an easy method for quantitative measurement of the slope. HARPI's provide an easy correspondence between echo and visual or photographic observations. However, the horizontal structure is distorted by the constant azimuth scale (tangential distances are variable).

With HARPI's and zero-degree PPI, the PPI gives a reference for compensation for the distortion of HARPI's and gives horizontal unity to them.

In summary, the CAPPI as a single display has the best comprehensibility. HARPI's are satisfactory, and when accompanied by one map-type picture they have the same degree of comprehensibility as CAPPI's, with some advantages and disadvantages.

b) Representativeness: CAPPI presentation does not convey the inherent limitations of the radar data such as the decrease in spatial resolution with range. Further CAPPI's are formed by annular slices of PPI's and therefore do not result in well-defined layers of space. The height of the beam centres vary with range. A linear antenna program such as that of the Alberta radar or the CPS-9 operating in Montreal yields layers of variable thickness, and there can be an overlap between them.

With HARPI's, the resolution of the pictures has the same variation with range as the radar beam. With elevation angles relatively small (20 degrees) the boundaries of the vertical slices are very close to being straight, which is just as they should be.

HARPI's with one PPI are as good as HARPI's alone.

The relative rating should be HARPI, good; CAPPI, poor.

c) Geographical representation is the correspondence between a map and the display, especially important for operational use.

CAPPI is excellent in this sense. It can be directly projected over a map.

With HARPI, the transformation from azimuth-height coordinates to rectangular coordinates is very difficult, although one single point is easily localized on a map on which polar coordinates are drawn. Another solution is a map in the same coordinates as the HARPI's on which these are projected, but this is not completely satisfactory.

HARPI with one PPI: The PPI compensates completely for this HARPI inconvenience.

In conclusion, HARPI's alone give poor geographical representation, but with one PPI they are as good as CAPPI's.

d) Completeness of the information available.

For CAPPI's, obtained with a linear antenna program, the variable thickness of the CAPPI layers leads to their overlapping at long ranges and gaps between them at short ranges. The amount of the gap decreases with the number of CAPPI layers but in a practical case there is some loss of information.

HARPI and HARPI with one PPI are complete, and should be rated as good, with the CAPPI's as satisfactory.

e) Compactness is measured by the area of film (or any storage element) which contains the data.

CAPPI's have a decreasing density of information with range which represents a waste of storage space. Also the circular frame is inefficient.

HARPI's utilize the entire surface of the film to present data with constant density of information.

HARPI's with one PPI are almost as good as HARPI alone.

HARPI's have the most efficient display from the compactness point of view and CAPPI is satisfactory.

f) Measurability refers to the facility with which quantitative information can be obtained from the display. Measurements of heights, areas of different shades as a function of height and slope are of interest.

CAPPI heights are easily limited, but with the accuracy depending on the number of maps. Areas are measured with a planimeter which is a simple though tiresome method. To measure the slope of a feature the

centre of it has to be determined in space at different elevations and the slope calculated after that stage has been reached.

HARPI heights are measurable with a scale beside the HARPI strips or by counting the horizontal lines and using an appropriate table. Areas are determined by measuring the azimuth extension at a given height, multiplying by $\frac{r\Delta r}{2\pi}$ and adding for all the ranges which contain the feature of interest. Slopes are easy to measure when they occur tangentially with respect to the radar. When they have a radial component, the same difficulty as with CAPPI is present (but is easier to appreciate).

With an appropriate overlay grid with height-azimuth lines for every range interval, HARPI's should be as easy to handle as CAPPI's, having the advantage of being easily adaptable for computing or for automatic measurements.

HARPI's with one PPI are as good as HARPI's alone.

It can be concluded that CAPPI's and HARPI's have good measurability characteristics.

Table 1 summarizes these estimations. The numbers 1-2-3 have been assigned to poor-satisfactory-good in that order. Assigning the same weight to all the characteristics the last row indicates the total rating of the presentations.

| | CAPPI | HARPI | HARPI + 1 PPI |
|---|---|---|---|
| Comprehensibility | 3 | 2 | 3 |
| Representativeness | 1 | 3 | 3 |
| Geographical Representation | 3 | 1 | 3 |
| Completeness | 2 | 3 | 3 |
| Compactness | 2 | 3 | 3 |
| Measurability | 3 | 3 | 3 |
| Totals | 14 | 15 | 18 |

Although the evaluation is very crude, a quite definite conclusion results from it. CAPPI's and HARPI's appear to be of comparable usefulness, and when the zero degree PPI is added to the HARPI's the combination results in the decidedly best display of information. These conclusions remain valid even with any of the rows of Table 1 removed.

## 11. Conclusions

Polar coordinates are the "natural" coordinates of the radar by its way of scanning the space. Also, the resolution in azimuth and elevation is constant in angle, at all ranges (limit equal to the beam width). Thus linear resolution across the beam varies with range (limit proportional to range) whereas linear resolution along the range is invariant with range. The amount of information obtainable per unit volume of storm decreases as the range increases. This very important characteristic is a limitation which tends to be forgotten when the data analysis is made using the current radar displays such as PPI, RHI or CAPPI. The HARPI display has a built-in reminder of this limitation: the variation with range of the resolution on the display is proportional to that of the radar beam. Thus with a constant density of information on the pictures, there is a loss of detail with range in accordance with the resolution capability of the radar. This is apparent on Fig. 4b where the diminishing size with range of the picture of the storm shows less detail. In the electronically produced HARPI's such as those of Figures 5, 6a and 7, the number of the elementary units per unit volume of the storm diminishes with range, and therefore the pictures faithfully represent the information available.

The density of information on a PPI, CAPPI or RHI picture diminishes with range (no matter how smooth the picture looks) and therefore a good part of the area of the picture is wasted. As was mentioned, HARPI's are produced with constant density of information, and on this account it is possible to display on a single HARPI picture the information contained in 20 PPI pictures (in the case of the Alberta radar). From the operational point of view this is very important because the HARPI display makes available in real time the complete storm situation presented in a very concise manner.

HARPI conveys information in the same coordinates as does the visual observation of the clouds from the radar site. The correspondence between such visual observations or cloud photography (which is part of the Alberta operation) is therefore facilitated.

Radar information has, at any given instant, four coordinates (three spatial and intensity). In presenting this information the following factors have to be taken into account: the completeness of the information for research use, the real-time delivery of the information for operational use, the clarity of the display and the correct emphasis on the relevant aspects of the storm. In Fig. 4b, in addition to the electronically generated CAPPI's, a hand-made HARPI was added; in Figs. 6, 14 and 18, hand-made maps were added to the HARPI's. It is clear that with both sections (horizontal and vertical) the understanding of the storm is much more complete and faster than with either of them alone, although the information contained in one of them is the same as that in the other. HARPI's alone lack the geographical representation and is difficult to establish continuity from one section to another. If, to the HARPI sections of Fig. 4b, only the 5 kft CAPPI map is added, the precipitation area is immediately located geographically and the storm acquires unity. Thus as a supplement to HARPI, one map is nearly as good as four; the utility of the single map increases with increasing experience. This can be seen also in Figs. 6a and 6b and Fig. 18. In every case the horizontal section does not add to the understanding of the three-dimensional structure of the storm, and therefore more CAPPI heights might still be advantageous for research purposes, as well as some RHI sections.

The presentation of the maximum signal, instead of the average, in a 2 nmi range interval (a characteristic of the Integrator and not necessarily of the HARPI display) overestimates the range extension of a particular feature. The relative importance of this error increases when the size of the observed feature decreases. This can be corrected by the systematic use of the values of $L_o$ given by expressions (15) and (15') if measurements of area, volume or water budget of a storm are made.

During the Alberta trials HARPI pictures were used operationally during every storm-occasion. The best and fastest understanding of the storm and its evolution was achieved when the HARPI pictures were used in conjunction with the zero-degree PPI's taken on Polaroid film. The good quantization of echo intensity, apparent on the pictures as sharply defined shades of grey, and the immediate display of vertical structure, permitted guidance of mobile crews under the desired zones of the storm. It was on this account, we hope, that the best hail samples were collected during the period in which the HARPI pictures were available.

The usual storm in the region of the Alberta Hail Studies (as revealed by the radar) is a cluster of cells, each approximately 5 nmi in diameter, the cluster covering an area of some 20 nmi in its maximum dimension. Therefore the total range of 28 nmi surveyed at one time was sufficient. On the other hand a resolution of 2 nmi made it difficult to distinguish individual cells if they were located radially with respect to the radar due to the small separation between cells.

It was found that beyond 50 nmi the additional information provided by the HARPI's was negligible. A storm having 5 nmi in diameter and 5 nmi in height is represented by 6 times 5 lines at that range; the internal structure cannot be revealed usefully with so few lines. Therefore the system was operated mainly at ranges between 50 and 10 nmi.

One general shortcoming of the HARPI presentation is that the storms are cross-sectioned by curved surfaces (cylinders). The departure from plane surfaces depends on the size of the storm in relation to its distance to the radar. Although there is no fundamental reason why one specific form of cross-section should be desirable (unless it is chosen at will for each occasion), a plane one offers the advantage of simplicity. This inconvenience of the HARPI's was made less in Alberta by the relatively small size of all the storms.

The long-term stability of the circuitry was very good, and little maintenance was required. The calibration of the thresholds remained practically unchanged during periods of a fortnight, which is a good indication of the over-all performance.

## REFERENCES

Atlas, D., 1947: "Preliminary report on new techniques in quantitative radar analysis of thunderstorms." Rept. AWNW-7-4, Pt. 1 Air Materiel Command, Dayton, Ohio.

Atlas, D., 1953: "Device to permit radar contour mapping of rain intensity in rainstorms." U.S. Patent No. 2656531. Also Re-issue Patent No. 24084, Nov. 1, 1955. U.S. Gov't. Printing Office, Washington, D.C.

Bartnoff, S., W.H. Paulsen and D. Atlas, 1952: "Experimental statistics in cloud and rain echoes." Proc. 3rd Weather Radar Conf., McGill Univ., Montreal, pp G1-G7.

East, T.W.R., and B.V. Dore, 1957: "An electronic constant-altitude display." Proc. 6th Weather Radar Conf., Am. Meteor. Soc., Boston, pp 325-330.

Henry, C.D., 1964: "High Radar Echoes from Alberta Thunderstorms." Scientific Report MW-39, McGill University Stormy Weather Group.

Hitschfeld, W., and A.S. Dennis, 1957: "Measurement and calculations of fluctuations in radar echoes from snow." Scientific Report MW-23, Stormy Weather Group, McGill University.

Holtz, C., 1968: "Life-Cycle of a Summer Storm from Radar Records." Scientific Report MW-55, McGill University Stormy Weather Group.

Jordan, C.L., 1961: "On the Maximum Vertical Extent of Convective Clouds Over the Central and Southeastern United States." Proc. of the Ninth Weather Radar Conference, pp 96-101.

Kodaira, N., 1959: "Quantitative mapping of radar weather signals." M.I.T., Dept. of Meteor., Weather Radar Res. Contract DA-36-039-Sc-75030, Res. Rep. No. 30, 39 pp.

Marshall, J.S., 1957: "The constant-altitude presentation of radar weather patterns." Proc. 6th Weather Radar Conf., Am. Meteor. Soc., Boston, pp 321-324.

Niessen, C.W., and S.G. Geotis, 1963: "A signal level quantizer for weather radar." Proc. 10th Weather Radar Conf., Am. Meteor. Soc., Boston, pp 370-373.

Smith, P., 1964: "Interpretation of the Fluctuating Echo from Randomly Distributed Scatterers: Part 3." Scientific Report MW-39, McGill University Stormy Weather Group.

Smith, P., 1966: "Interpretation of the Fluctuating Echo from Randomly Distributed Scatterers: Part 3." Proc. Twelfth Conference on Radar Meteorology, pp 1-6.

Sweeney, H.J., 1961: "The weather radar data processor." Proc. 9th Weather Radar Conf., Am. Meteor. Soc., Boston, pp 372-378.

Wein, M., 1963: "Facsimile output for weather radar." Proc. 10th Weather Radar Conf., Am. Meteor. Soc., Boston, pp 365-369.

Wein, M., 1965: "Facsimile and areal integration for weather radar." Scientific Rep. MW-40, Stormy Weather Group, McGill University.

APPENDICES


| | | |
|---|---|---|
| 1 | Resolution requirements of film and CRT | 61 |
| 2 | Delay | 63 |
| 3 | Oscillator | 65 |
| 4 | Sampler | 67 |
| 5 | Counter | 69 |
| 6 | Store | 71 |
| 7 | Divide-by-8 | 73 |
| 8 | Erase | 74 |
| 9 | Thresholding Amplifier | 76 |
| 10 | Elevation Shift Generator | 78 |
| 11 | Range Time Base | 80 |
| 12 | Azimuth Time Base | 82 |
| 13 | Assembly of components | 85 |


Note: In the following circuit diagrams all NPN transistors are 2N3643; all PNP transistors are 2N3638; all FET are 2n4343; all resistors are given in K$\Omega$ (rated at 1/4 W dissipation) and capacitors in $\mu$F unless otherwise specified.

Appendix 1

Resolution requirements of film and CRT

For a HARPI section the shape factor between horizontal and vertical scales is constant with range, and it was arranged to be 2:1 in our case. On the other hand the elementary units in our pictures correspond to 1 degree in elevation and 0.8 degrees in azimuth. Therefore the factor between the horizontal and vertical dimensions of this unit is:

$$\text{(shape factor) x (angular dimension factor)} = 2 \times \frac{1}{0.8} = 2.5$$

Thus the height of the elementary units is 2.5 times its width. Therefore the resolution requirements of the CRT and the film are set by the number of lines to be displayed in the horizontal direction. In the case of the Alberta radar this number was 450 (corresponding to 8 rpm of the antenna and 60 sweeps per second coming out of the integrator).

With 14 range intervals and 20 lines in each, the total number of lines to be displayed in the vertical is 280. Because these lines are 2.5 times higher than their width, they require a space equivalent to 700 lines. Accordingly the shape of the picture was set by the ratio 700:450 = 1.55.

The CRT used (Thomas Electronics, Inc. Type 5M45P11M) has a face-plate of 5" and a line width of 0.0015 inches or 26.7 lines per mm. Therefore it is capable of displaying 2120 lines in 8 cm, that is about 3 times the number required presently. Probably it could be used to display twice the present number of range intervals, still leaving some "safety" factor.

The photographic camera used (Tektronix type C27) produced a magnification of 1.1 on the film. Therefore the resolution required on it is about the same, and the Polaroid film easily satisfied this requirement.

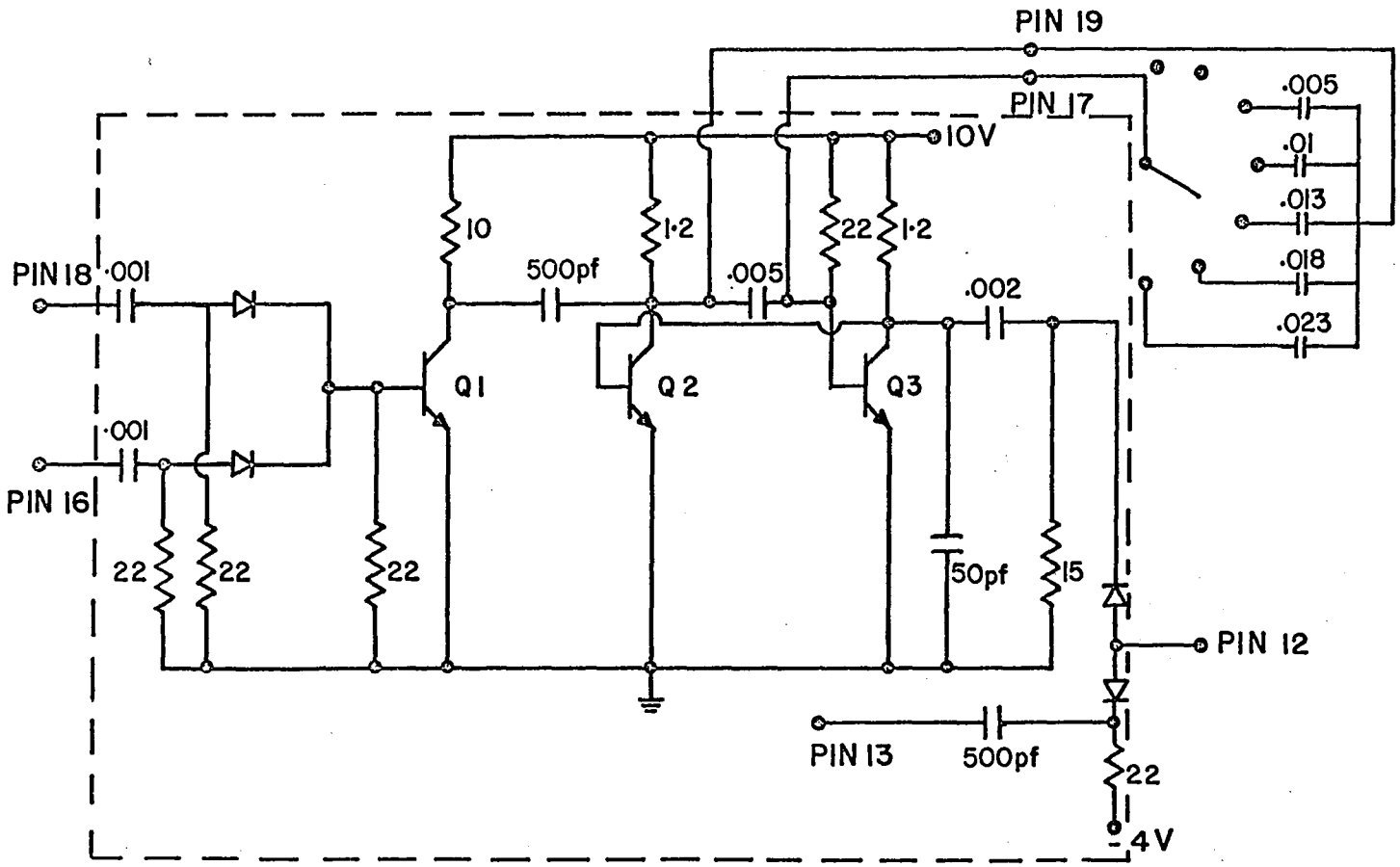


C 5 PIN 18: GATE FROM ERASE

C 5 PIN 16: RADAR TRIGGER

C 5 PIN 13: PULSES FROM SAMPLER

C 5 PIN 12: TO COUNTER TRIGGER BUFFER

FIG. A 2: DELAY

Appendix 2

Delay

(1) Produces a pulse delayed from the radar trigger which thereafter is used to initiate the process of integration.

(2) After 8 radar pulses it is also triggered by the Erase pulse to initiate the action of the Oscillator and the Counter, and therefore the discharge cycle of the capacitors. Thus there is a delay between the beginning of gate 16 and the start of the erase which is equal to the minimum range of integration.

The circuit is shown in Fig. A2. It is basically a monostable with adjustable capacitor coupling between the collector of $Q_2$ and base of $Q_3$. The two first positions of the switch correspond to a minimum range of 10 nmi (for range intervals 5 nmi and 2 nmi). The others correspond to 5 nmi increments up to 35 nmi (for range interval 2 nmi).

Inputs: Radar trigger

A positive Erase gate

Output: A trigger to the Counter

Power requirements: +10 V

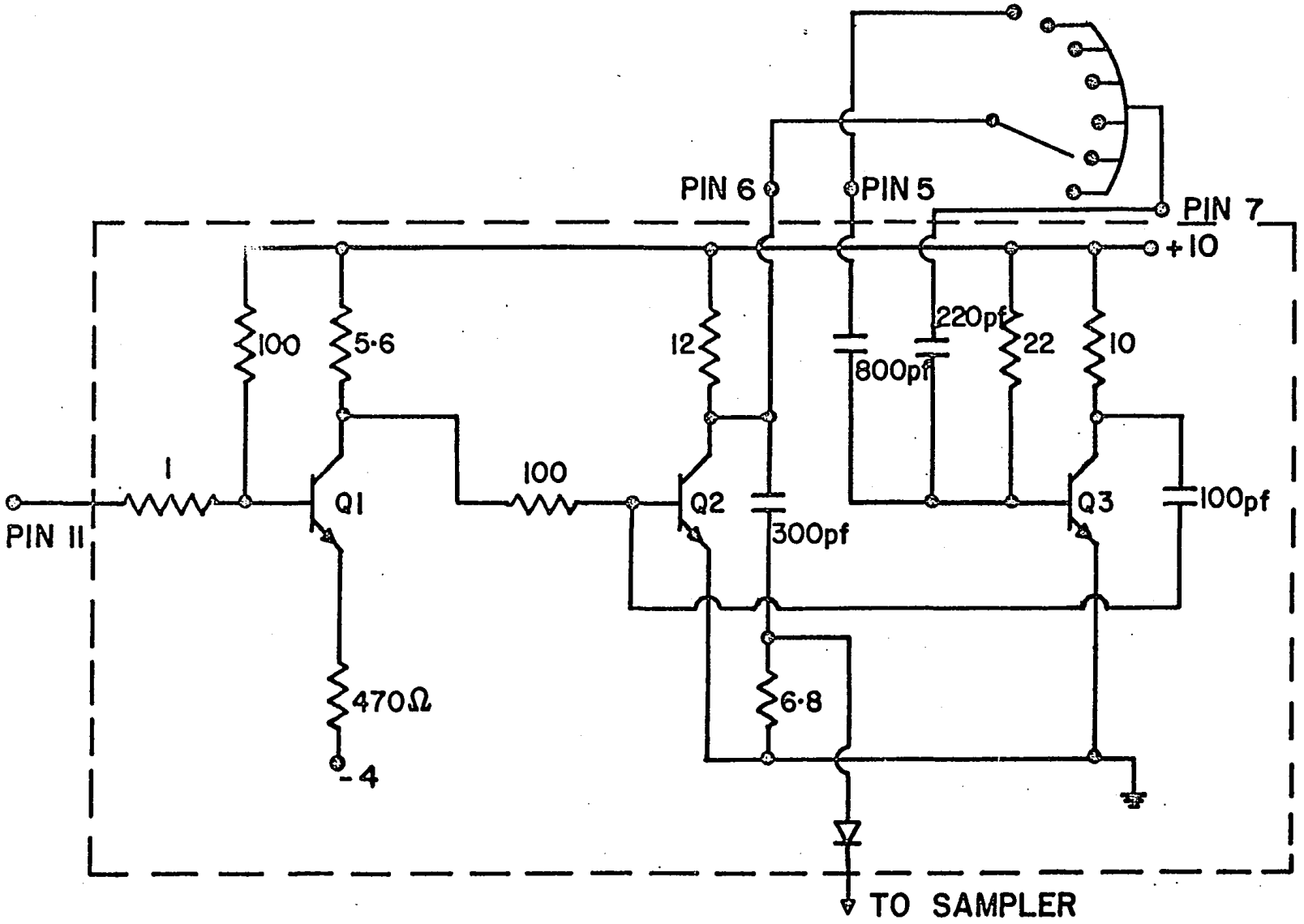


PIN 11: FROM GATE 16

FIG. A3: OSCILLATOR

Appendix 3

Oscillator

The function of the Oscillator is to provide 15 pulses after the delayed pulse, to trigger the Sampler. Pulse No. 15 produces gate 16 from the Counter which inhibits the Oscillator. It remains off until gate 16 is removed by a trigger from the Delay.

The period of oscillation is adjustable to two values, 25.2 $\mu$sec and 63 $\mu$sec corresponding to 2 nmi and 5 nmi. In Fig. A3, transistors $Q_2$ and $Q_3$ form an astable multivibrator with its frequency controlled by the value of the capacitor that couples the collector of $Q_2$ to the base of $Q_3$. The base of $Q_2$ is connected through a 100 K$\Omega$ resistor to the collector of $Q_1$. The base of $Q_1$ is connected to gate 16 from the Counter, which is at -4V during Counter operation and at ground level after all the other gates have been produced. Therefore $Q_1$ is not conducting unless gate 16 is present and the 100 K$\Omega$ resistor to the base of $Q_2$ is at +10 V: $Q_1$ is turned on by gate 16 and the 100 K$\Omega$ resistor to the base of $Q_2$ drops below ground stopping the action of the Oscillator.

The output is taken from the collector of $Q_2$ and is differentiated to provide trigger pulses.

Input: Gate No. 16 from the Counter

Output: Set of 15 pulses to trigger the Sampler

Power requirements: +10 V; -4 V

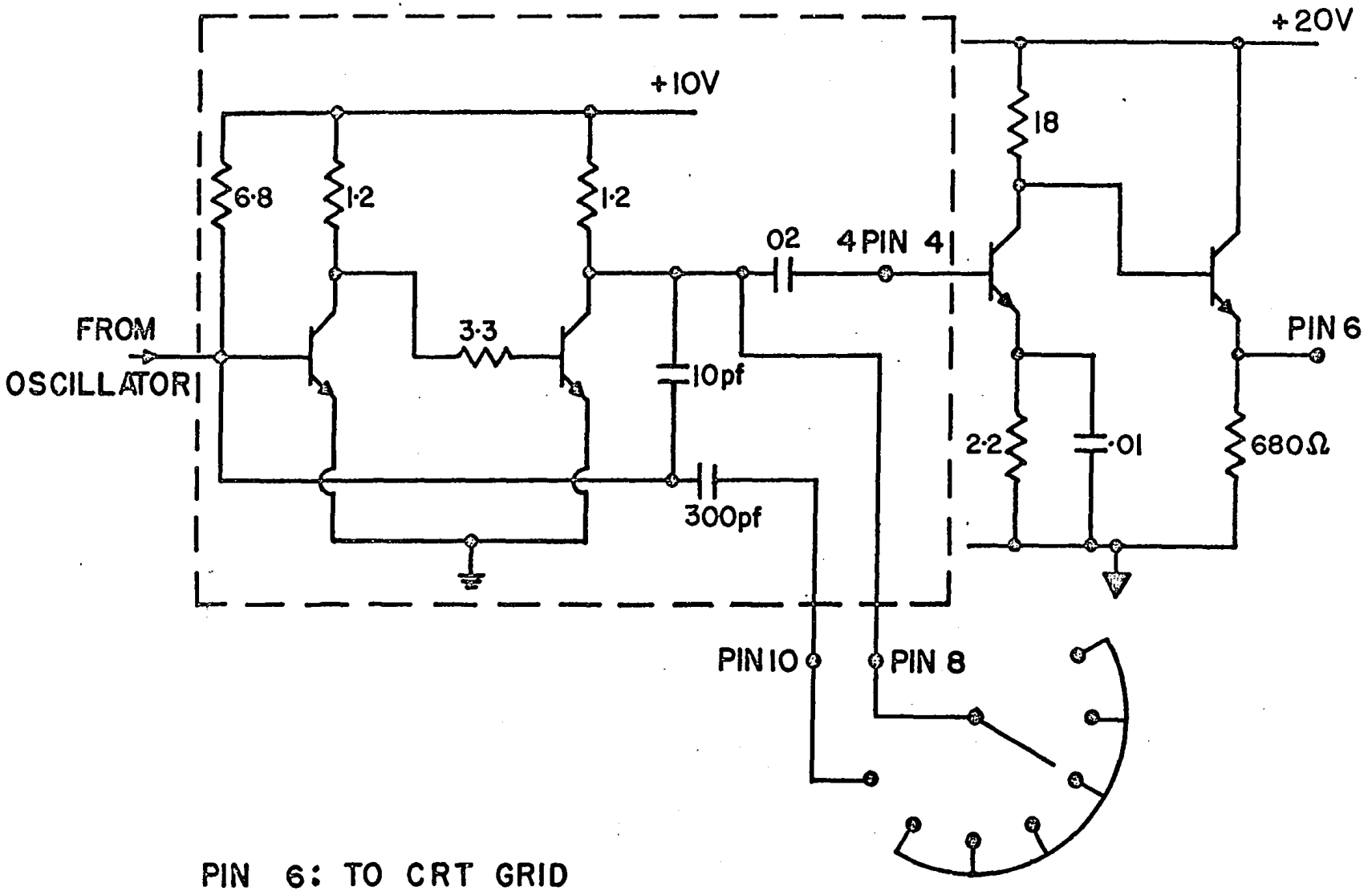


FIG. A4: SAMPLER

Appendix 4

Sampler

This sub-unit provides essentially rectangular pulses to brighten up the CRT during 1/20 of every range interval. Because it is desired that the sampled fraction of the range interval occur at the end of it, the trailing edge is used to trigger the Counter. Thus a new gate is produced after the end of each Sampler pulse.

The circuit diagram of Fig. A4 shows the Sampler. It is composed of a monostable multivibrator and a pulse amplifier. An emitter follower couples it to the grid of the CRT.

The note under (b) of picture limitations points out that the Sampler pulses are not in fact rectangular. Further development is needed to reduce the switching time and lower the output impedance of this circuit.

Input: trigger pulses from the Oscillator

Output: Rectangular pulses with adjustable width to two values:

1.2 $\mu$s and 3.1 $\mu$s

Trigger pulses for the Counter

Power requirements: +10 V; +20 V

Notice in Fig. A4 that two ground levels are indicated. The one indicated by the arrow is 35 V below the other and is the central tap of the power supplies feeding the deflection amplifiers. This arrangement will appear every time there is need to show the common ground together with CRT circuits.

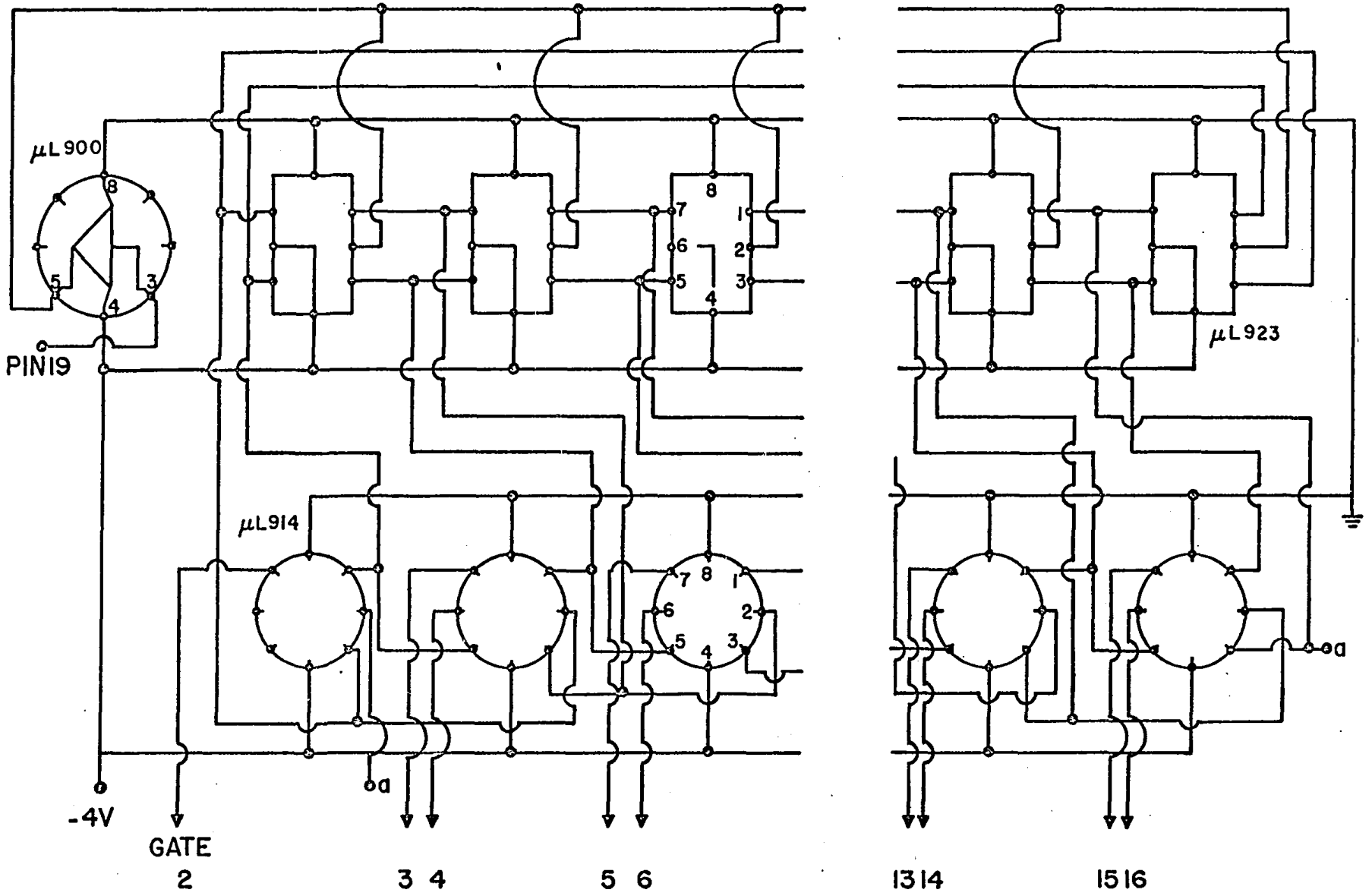


PIN 19: TRIGGER FROM DELAY AND SAMPLER

FIG. A5: COUNTER

Appendix 5

Counter

The purpose of this sub-unit is two-fold:

(1) It generates the gates for the switching transistors

(2) At the end of each switching cycle it stops the action of the Oscillator.

It is composed of 8 flip-flops and 8 dual AND gates (Fairchild RT micrologic integrated circuits series $\mu$L923 and $\mu$L914). The configuration used is indicated on Fig. A5. All the flip-flops are triggered simultaneously by a buffer ($\mu$L900) avoiding propagation delays.

The first trigger to the Counter comes from the Delay and the remaining 15 from the Sampler. Therefore the length of the first gate is not set by the Oscillator and is not used as range gate.

Input: Trigger pulse from the Delay followed by
15 pulses from the Sampler

Output: 14 gates to the switching transistors of the capacitor Store and a gate to inhibit the Oscillator

Power requirement: -4 V

Note that the Counter operates 9 times every 8 radar pulses, the 9th operation being the Erase cycle.

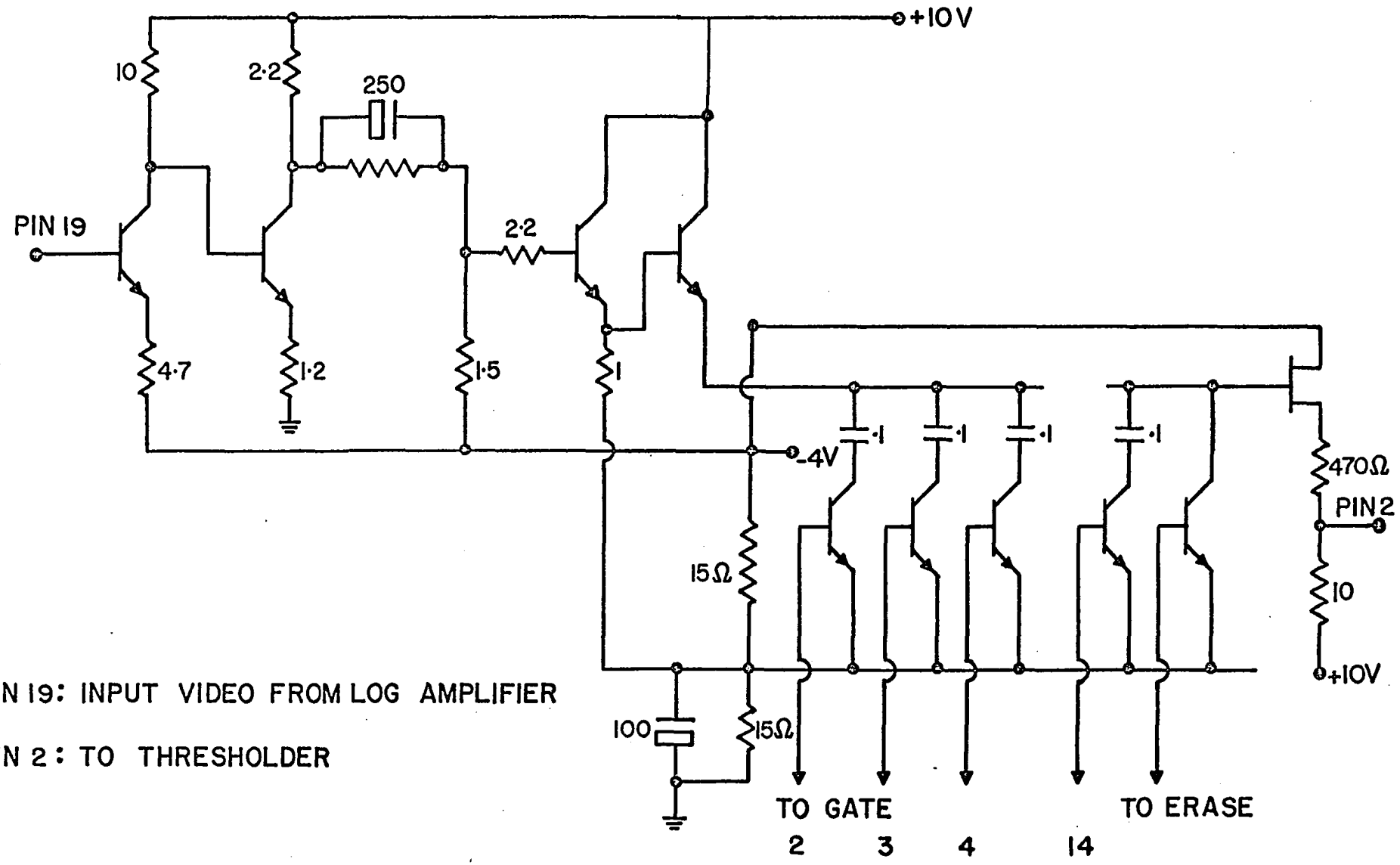


PIN 19: INPUT VIDEO FROM LOG AMPLIFIER

PIN 2: TO THRESHOLDER

FIG. A6: STORE

Appendix 6

Store

As shown in Fig. A6, the Store is composed of 14 capacitors connected to the video through a two-stage emitter follower. The other end of each capacitor is connected to the collector of a transistor switch. All 14 emitters are biased to -2.0 V. In this condition the transistors are fully turned on and off by a gate going from -4 V to 0 V provided by the Counter. Another switching transistor connected between -2.0 V and the common terminal of the capacitors acts as a discharge path when a gate from the Erase is applied. The output stage is a FET connected as a source follower.

Inputs: Video signal in logarithmic scale from a log amplifier
Fourteen gates from the Counter
A gate from the Erase

Output: Integrated video to the Threshold Amplifier

Power requirements: -4 V; +10 V

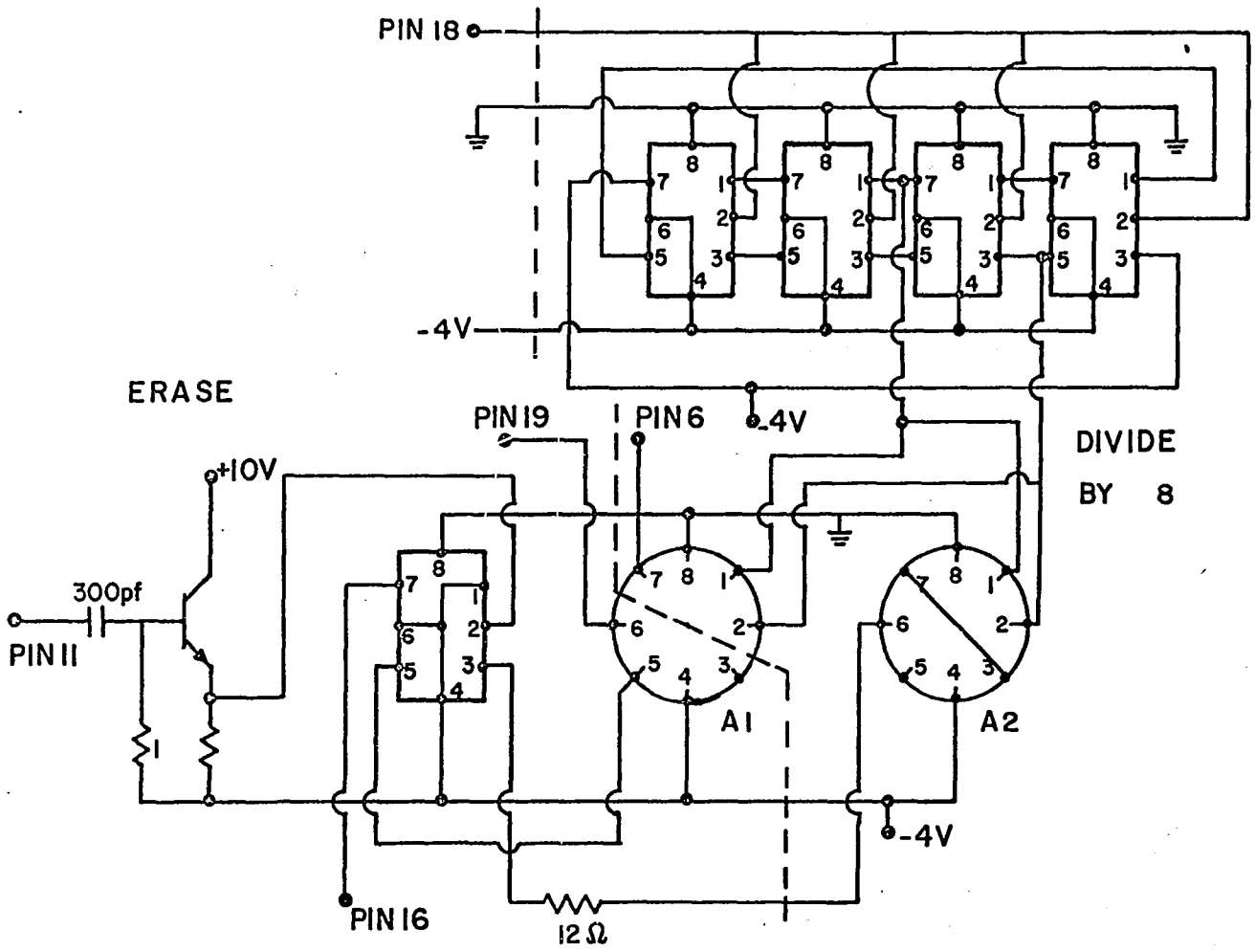


PIN 11: FROM GATE 16

PIN 19: GATE TO ERASE TRANSISTOR

PIN 16: TRIGGER TO DELAY

PIN 6: RANGE TIME BASE TRIGGER

PIN 18: RADAR TRIGGER

FIG. A7: DIVIDE—BY—8 AND ERASE

Appendix 7

Divide-by-8

Its purpose is three-fold:

(1) Provide a trigger to initiate the range time base at the eighth radar pulse

(2) Hold off for 7 radar pulses the Erase flip-flop which otherwise would erase the Integrator after every pulse

(3) To trigger the Azimuth Time Base charging monostable.

It is a synchronous counter composed of 4 flip-flops and one and a half dual AND gates (Fairchild RT micrologic integrated circuits series $\mu$L923 and $\mu$L914). Fig. A7 illustrates the configuration used. Half of the dual AND gate A1 is used to provide the trigger to Range Time Base. AND gate A2 produces an inverted pulse to hold off the Erase (coupled through a 12 resistor).

Input: Radar trigger

Output: One gate after the 8th pulse to the Range Time Base and azimuth monostable

One gate lasting for 7 radar pulses to the Erase flip-flop.

Power requirements: -4 V

Appendix 8

Erase

Provides after the 8th radar pulse:

(1) A gate to close the erase transistor switch

(2) A trigger to the Delay, thus initiating the Counter and the discharge of the capacitors.

It is a single flip-flop (Fairchild $\mu$L923) triggered by gate 16 through an emitter follower and held off by the Divide-by-8 (see Fig. A7). The positive going output is used to trigger the Delay, and the negative going output is inverted by an AND gate and used as the erase gate. The reason for using the AND gate inverter is to provide a gate to the erase transistor from a source which is identical to that supplying the switching transistors.

Input: Inhibiting gate from Divide by 8

Trigger from gate 16

Output: Two identical gates, one as a trigger to the Delay, the other to the erase switching transistor

Power requirements: -4 V; +10 V

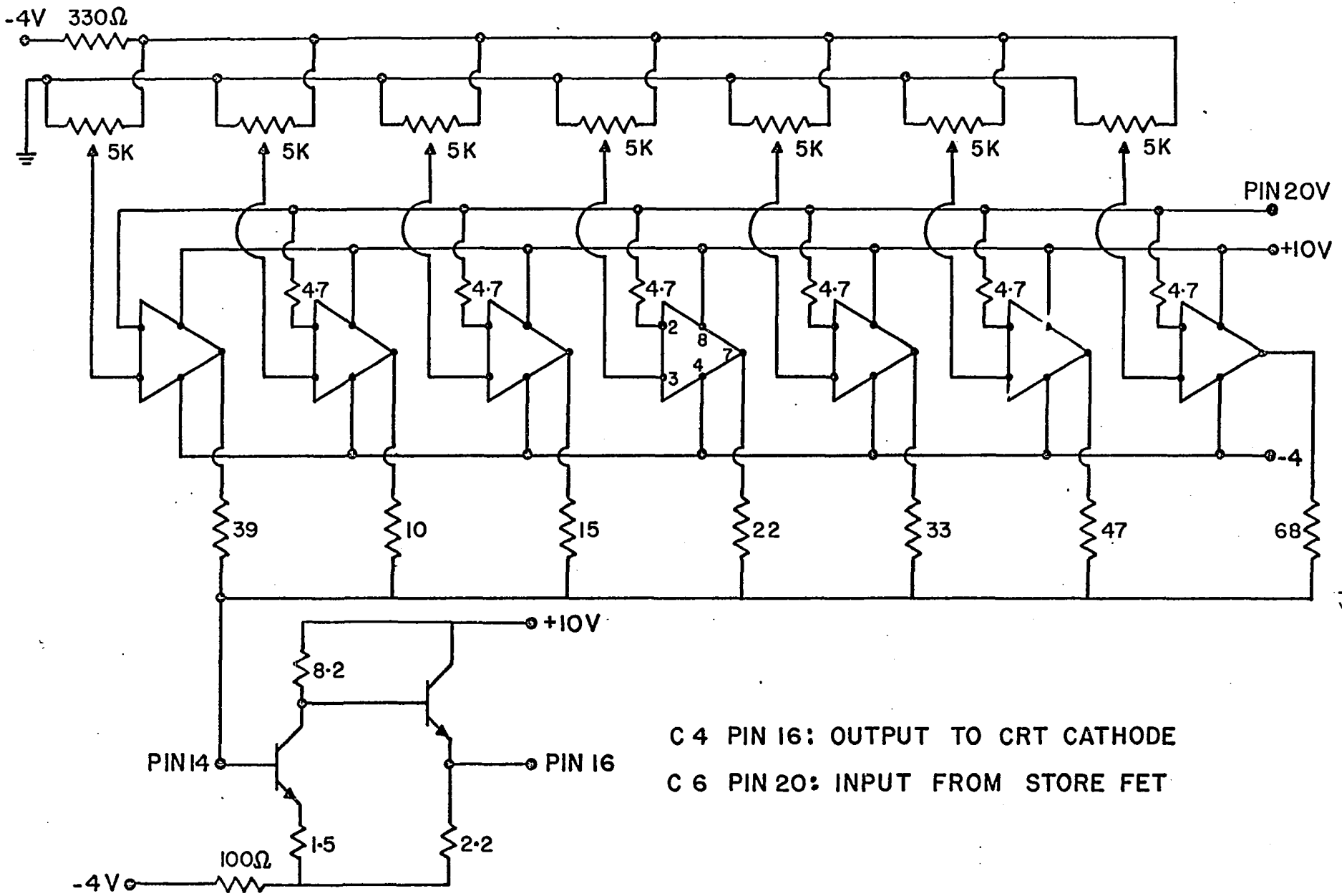


C 4 PIN 16: OUTPUT TO CRT CATHODE

C 6 PIN 20: INPUT FROM STORE FET

FIG. A9: THRESHOLD AMPLIFIER

Appendix 9

Threshold Amplifier

Quantizes the integrated video in 7 steps. The separation between levels is 10 db, although it is adjustable to any other value.

It is composed of 7 differential voltage comparators (Fairchild linear integrated circuit type $\mu$A 710C) as indicated in Fig. A9. The "inverting" input is connected to a fixed reference voltage (adjustable by the position of the 5K$\Omega$ potentiometers) and the "noninverting" input is connected to the output of the Store. The output summing network is non-linear, producing an antilog scale in the output voltage of the thresholds. This produces an approximately linear scale of brightness on the pictures. The value of the first resistor sets the contrast between shade 1 and background. A dc coupled video amplifier forms the output stage.

Input: integrated video from the FET of the Store

Output: quantized video to the cathode of the CRT

Power requirement: -4 V; +10 V

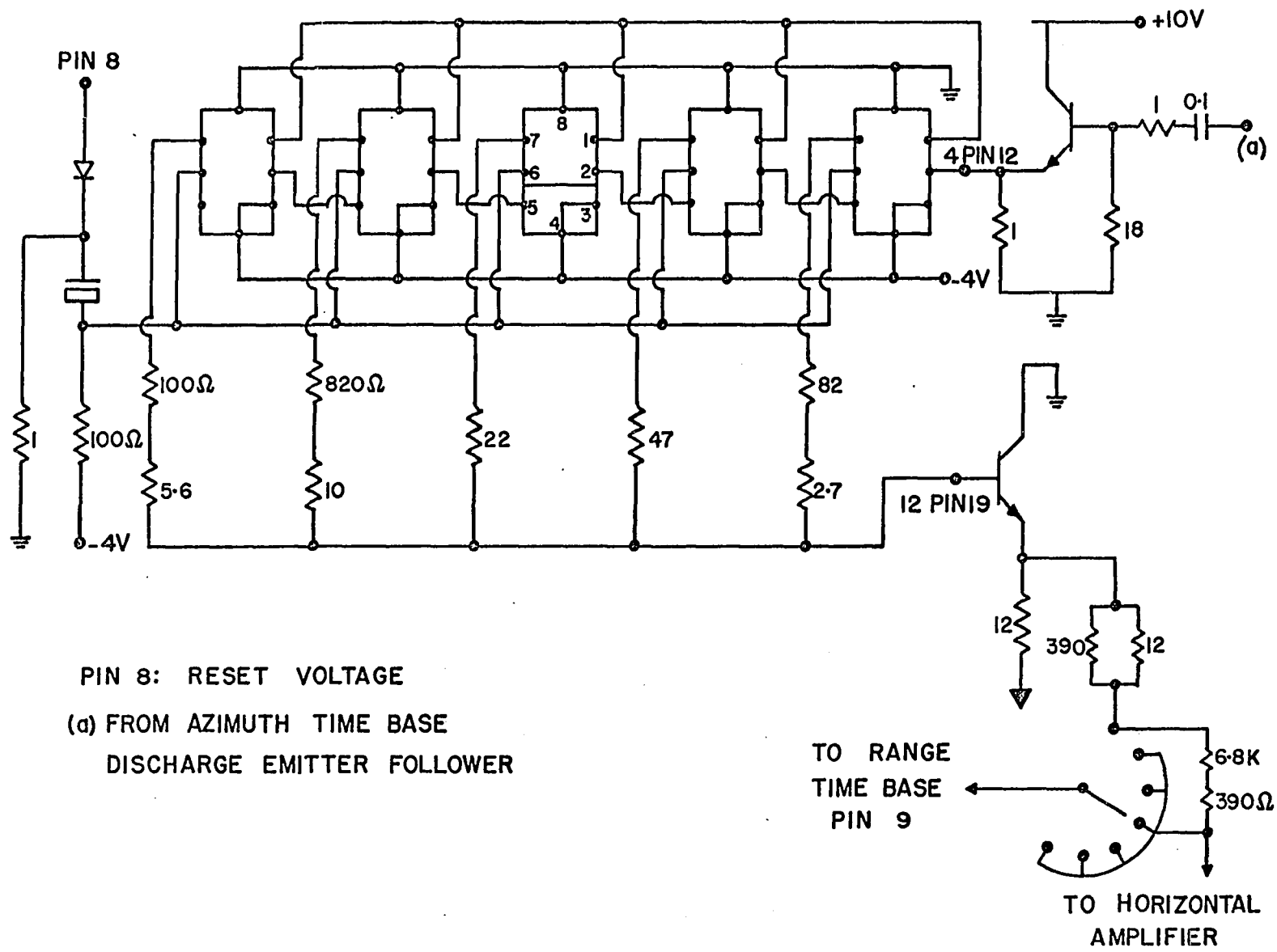


PIN 8: RESET VOLTAGE

(a) FROM AZIMUTH TIME BASE DISCHARGE EMITTER FOLLOWER

FIG. A 10: ELEVATION SHIFT GENERATOR

Appendix 10

Elevation Shift Generator

Produces an increase in the dc level of the Y deflection of the CRT, after every antenna rotation. In this way the location on the screen of the pulses from the Sampler is shifted along in the direction of increasing range, thus producing the scale of height.

It consists of a binary asynchronous counter and a summing network. The counter is built using 5 flip-flops (Fairchild RT micrologic integrated circuit series $\mu$L923). Every antenna rotation, a pulse from the Azimuth Time Base triggers the Counter. An emitter follower is needed to trigger the flip-flops. At the end of the antenna elevation cycle the counter is reset to zero by a voltage to pin 8 from a relay contact.

The summing circuit is composed of resistors in the sequence $R_n = \frac{R(n-1)}{2}$, where n is the flip-flop number (1 to 5). The circuit diagram is shown in Fig. A10. The output stage is an emitter follower coupling the staircase to the horizontal amplifier.

In spite of careful selection of the summing resistors, some inequality in step amplitude persisted, giving rise to the criticism mentioned under (c) of limitations.

Use of an elevation pick-off potentiometer in tests with the CPS-9 at Montreal airport has cured the problem. This entire circuit can be replaced next year by a single elevation angle pick-off potentiometer.

Input: trigger pulses every antenna rotation from the Azimuth Time Base

reset pulses after every antenna elevation cycle

Output: staircase voltage to horizontal deflection amplifier

Power requirement: -4 V; the output emitter follower is connected between ground and -35 V

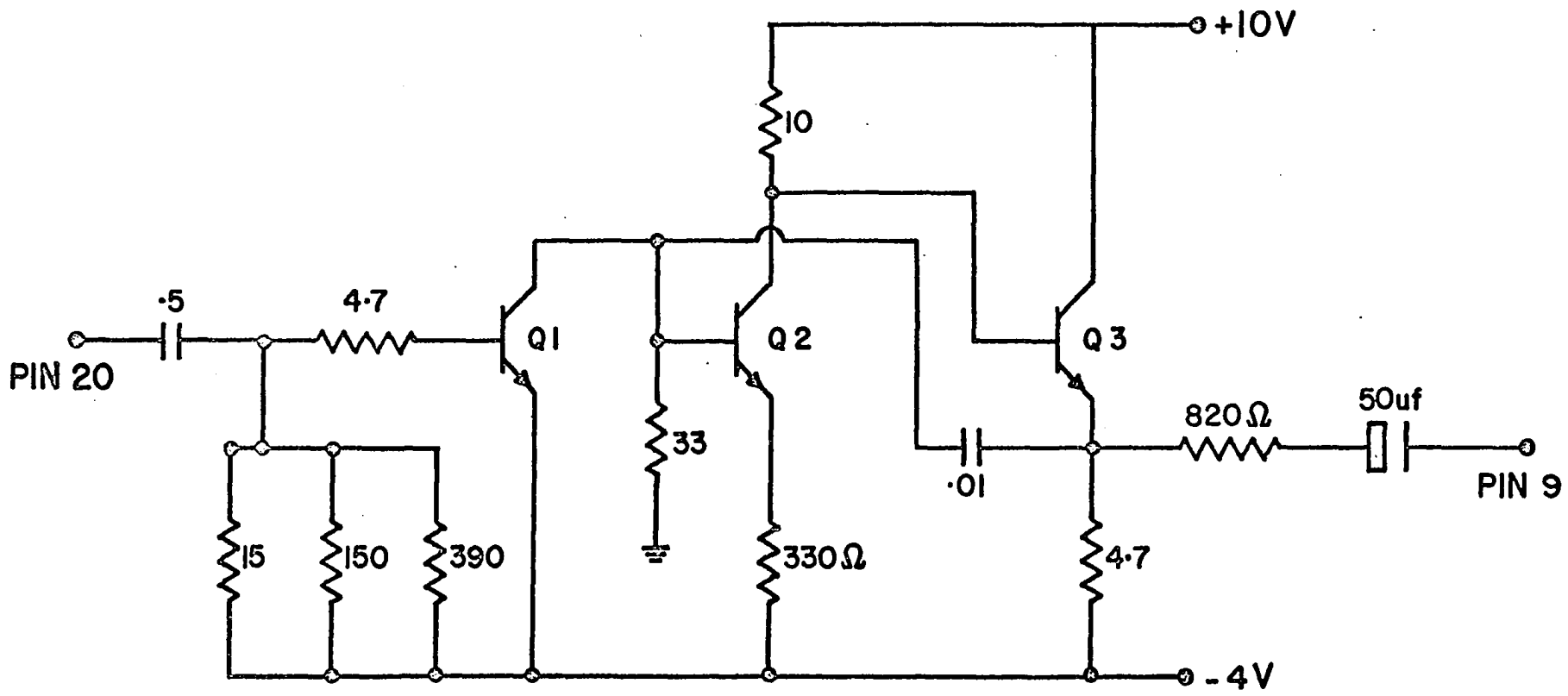


PIN 20: ENABLING GATE FROM DIVIDE — BY — 8

PIN 9: TO SUMMING POINT ELEVATION SHIFT GENERATOR

FIG. A11: RANGE TIME BASE

Appendix 11

Range time base

The circuit of Fig. All is a Miller integrator consisting of an amplifier (transistor Q2) and an emitter follower output state (transistor Q3). A negative gate from the Divide-by-8, connected to pin 20, is used to remove a cut-off bias from the amplifier which is imposed via the clamping transistor Q1. Miller action then takes place with time constant 33 K$\Omega$ x 0.01 $\mu$F.

In order to end the time base before the erase gates are generated, the Divide-by-8 gate is shortened by use of a differentiating circuit preceding the clamping transistor Q1. The amplitude of the range waveform to the elevation shift summing point is determined by the 820$\Omega$ series output resistor.

Input: Gate from Divide-by-8

Output: A ramp waveform

Power requirements: +10 V; -4 V

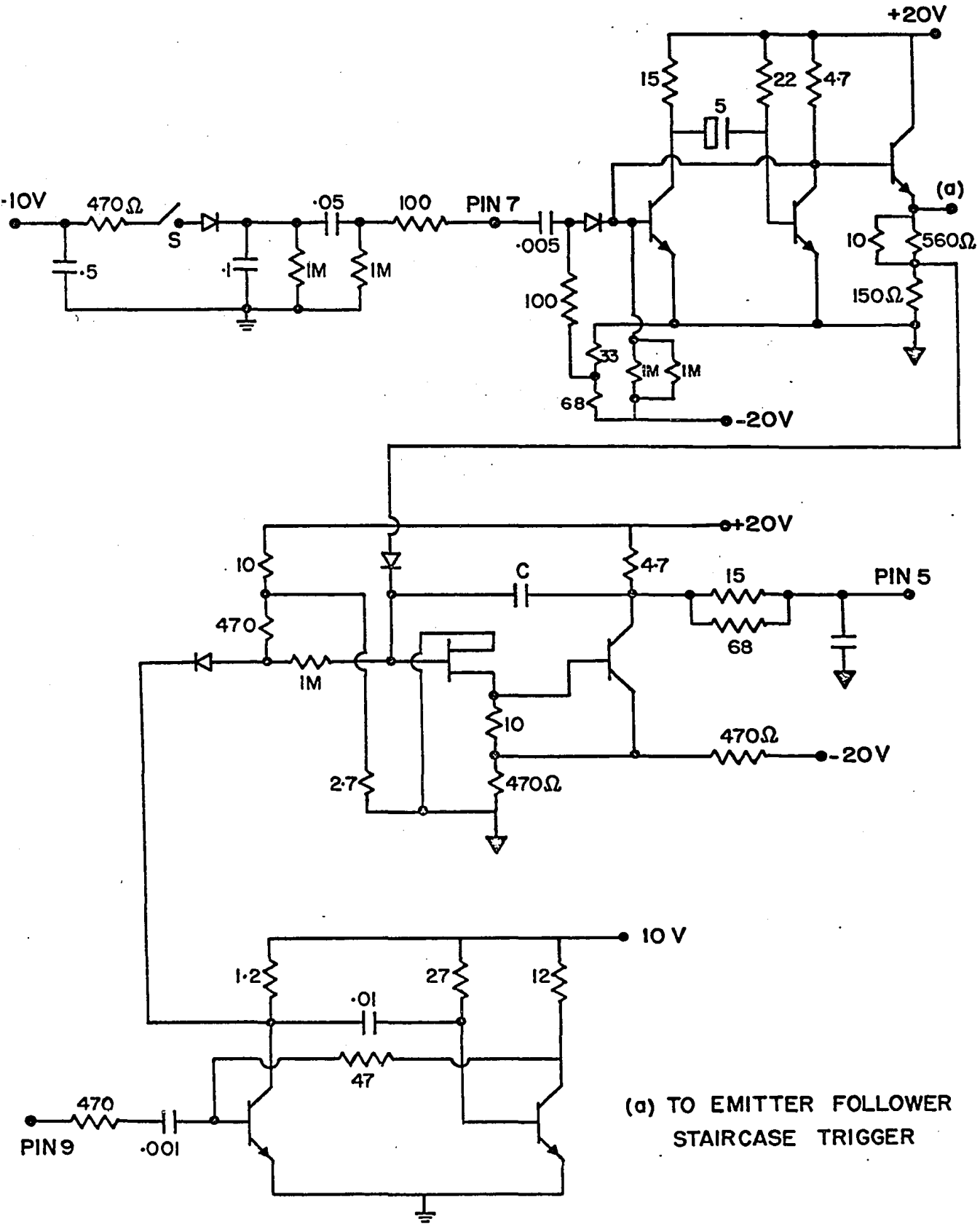


(a) TO EMITTER FOLLOWER STAIRCASE TRIGGER

FIG. A12: AZIMUTH TIME BASE

Appendix 12

Azimuth time base

As is shown on Fig. A12 this sub-unit is composed of 3 circuits: the central time base generator; charging monostable multivibrator (bottom of diagram); discharging monostable multivibrator (top of diagram). Positive going gates from the Divide-by-8 trigger the charging monstable which in turn produces pulses 100 $\mu$sec in width and 10 V in amplitude. These pulses charge the capacitor C(0.05 $\mu$F). Therefore the voltage across this capacitor increases every time the Integrator is read out. An FET and emitter follower form a miller feedback amplifier, the output of which is the azimuth deflection voltage. The charging pulse amplitude is chosen in relation to the output amplitude such that the resulting time base has good linearity.

Once each rotation of the radar antenna, the switch S in the discharging multivibrator is closed, and it produces a short pulse which discharges C, thus restarting the time base pulse. The same pulse is used to trigger the elevation shift generator. This entire circuit can be replaced next year by a single azimuth angle pick-off potentiometer.

Inputs: Trigger from Divide-by-8

Azimuth rotation switch closure

Outputs: stepwise increasing voltage to the vertical deflection amplifier

Trigger Pulse to Elevation Shift generator

Power requirements: +20 V; -20 V

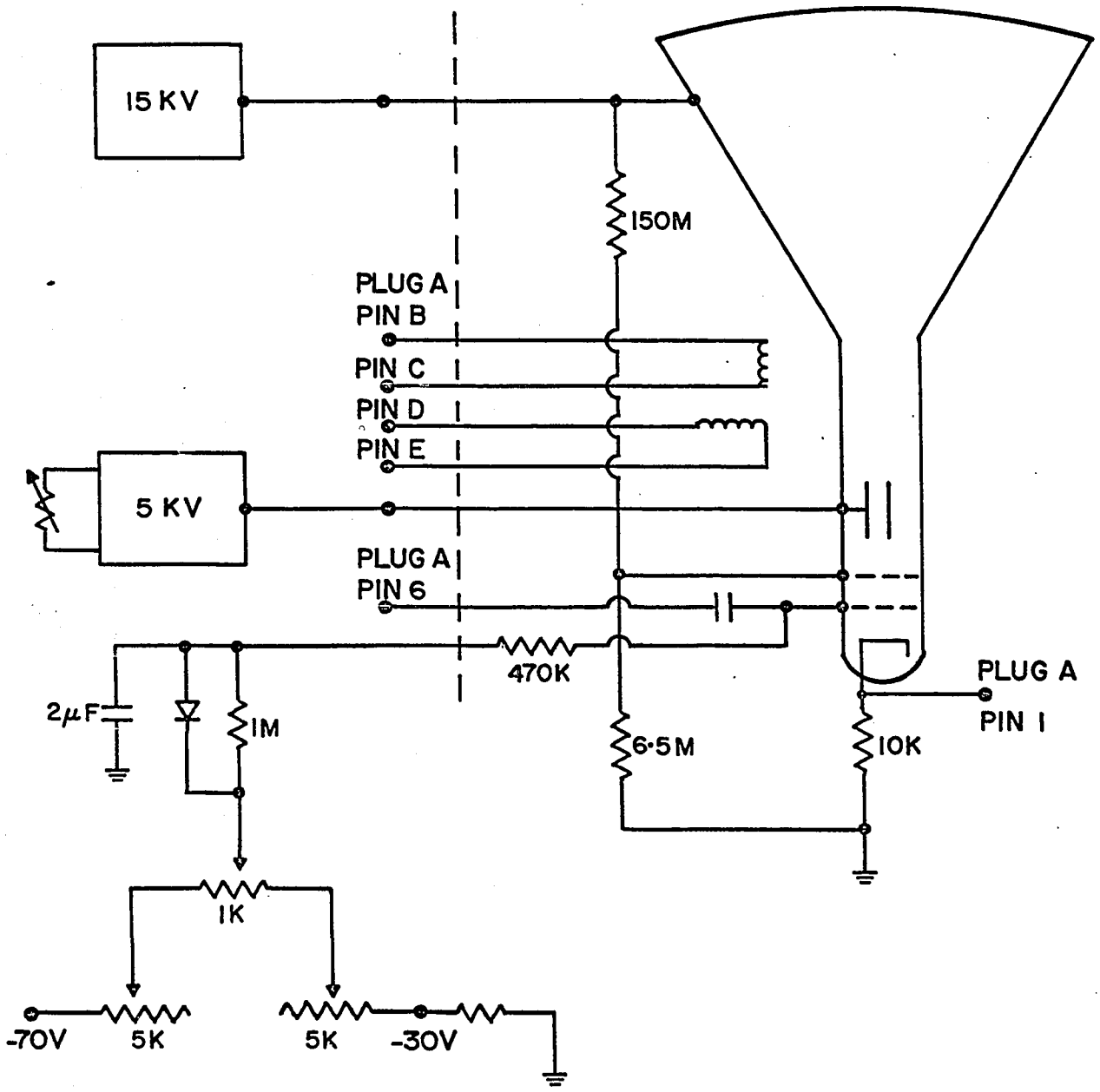
15 KV
150M
PLUG A
PIN B
PIN C
PIN D
PIN E
5 KV
PLUG A
PIN 6
470K
PLUG A
PIN 1
2μF
1M
6·5M
10K
1K
-70V
5K
5K
-30V

FIG. A13 a

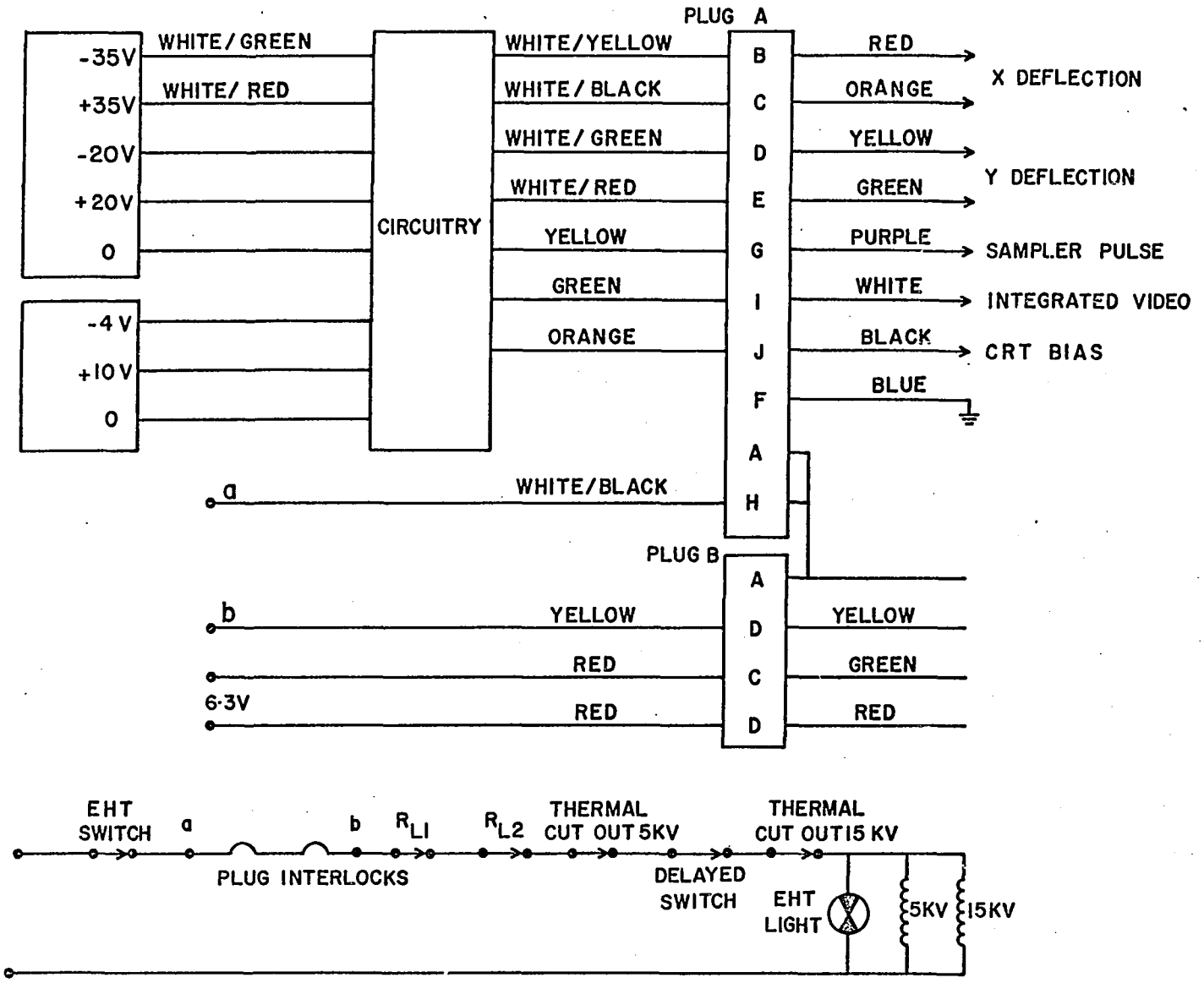
PLUG A
-35V
+35V
-20V
+20V
0
-4V
+10V
0
WHITE/GREEN
WHITE/RED
CIRCUITRY
WHITE/YELLOW
WHITE/BLACK
WHITE/GREEN
WHITE/RED
YELLOW
GREEN
ORANGE
B
C
D
E
G
I
J
F
A
H
RED
ORANGE
YELLOW
GREEN
PURPLE
WHITE
BLACK
BLUE
X DEFLECTION
Y DEFLECTION
SAMPLER PULSE
INTEGRATED VIDEO
CRT BIAS
a
WHITE/BLACK
PLUG B
A
D
C
D
b
YELLOW
RED
6·3V
RED
YELLOW
GREEN
RED
EHT SWITCH
a
b
$R_{L1}$
$R_{L2}$
THERMAL CUT OUT 5KV
THERMAL CUT OUT 15 KV
PLUG INTERLOCKS
DELAYED SWITCH
EHT LIGHT
5KV
15KV

FIG. A13b

Appendix 13

Assembly of components

The circuits which have been described were wired on 7 cards. A special card (Avnet H5936) was used for the integrated circuits and standard perforated boards for the discrete components. All cards were mounted on 22 pin sockets. This being an experimental model, many of the auxiliary circuits were added during the construction which has resulted in some disorderly location of the parts.

Two extra boards containing the deflection amplifiers (Beta Instrument Corp., Model DA341) complete the circuitry, which is mounted inside a cabinet together with the power supplies. All the control knobs (brightness, focus, minimum range of integration, thresholds of the grey scale) are located on the front of the cabinet. The access to the different pins of the cards is at the rear.

The high resolution CRT used (Thomas Electronics Inc., Type 5M45P11M) is mounted in a custom made frame and covered with a metal shield (Beta Instruments MS983) to avoid interference from external fields. The focusing of the tube is electrostatic while the deflection is magnetic. The deflection coils used are Syntronic Instruments Inc. Type Y58-DD-6S P/N C3301-5. Fig. A13a shows the CRT connections, and Fig. A13b shows the interconnections inside the cabinet and the power switching.

The note under (a) of limitations refers to a random deflection motion in the display.

A re-examination of the stability of power supplies and deflection circuits is required.